POLITECNICO
MILANO 1863

SCHOOL OF CIVIL, ENVIRONMENTAL AND LAND MANAGEMENT ENGINEERING
MASTER OF SCIENCE IN ENVIRONMENTAL AND LAND PLANNING ENGINEERING

DRIVERS OF UNCERTAINTY, HIGH-RISK SCENARIOS, AND ROBUST CLIMATE POLICIES IN RICE50+

Master Thesis by:
Luca Ferrari
Matr. 928442

Advisor:
Prof. Andrea Castelletti

Co-Advisor:
Angelo Carlino
Dr. Paolo Gazzotti

Academic Year 2020 – 2021

Acknowledgments

First of all, I would like to thank Prof. Andrea Castelletti for giving me the terrific opportunity to discover and work on this amazing topic, as well as for his advice and guidance. I really enjoyed diving into the topics of IAMs, climate change and economic inequality.
I will never thank enough my co-advisors, Angelo and Paolo, for the invaluable help they constantly gave me in these last months. Every aspect of this thesis owes a lot to their support, their patience, and their advice.
Special thanks go to my dear friend Riccardo. Our (mostly pacific) discussions about theories, coding and the usefulness of what we do are always enlightening.
I also wish to thank Giovanni, Ruggero, Loris, Simone, Aurora, Carolina, Giorgio and Davide, as well as all the other friends that are and will always be by my side. A big thanks also to Silvia for all the advice that I hardly ever listened to.
I am deeply grateful to my parents, my brother and my family for their advice, their guidance and their constant support in this long and challenging journey I undertook here at Politecnico.
Last but not least, a special thank you to Mary for sharing with me every moment, for keeping my feet on the ground when I stress out too much and for making my life the most wonderful adventure.

Abstract

Greenhouse gas emissions from human activities have been influencing the climate at an unprecedented rate, and temperature rise may lead to several impacts over the entire world. Contrasting anthropogenic climate change requires urgent mitigation actions. In this context, Integrated Assessment Models represent a helpful and influential tool. These models link climate, energy, and economic features in one framework and are used to search for Benefit-Cost optimal climate policies. Among these models, RICE50+ has recently introduced higher geographical resolution and better consideration for economic inequality. This thesis contributes to the analysis of the Benefit-Cost solutions of this model (i.e., the optimal emission reduction pathways). In particular, we addressed the identification of high-risk scenarios and robust optimal solutions. We started with the re-simulation of the solutions over a set of plausible future scenarios defined by the most relevant drivers of uncertainty of the model: the socioeconomic baselines, the climate impact functions and the Land-Use emission cases. Result performances have been measured for the objectives of welfare, temperature, and economic inequality. Then, we applied a scenario discovery algorithm to identify which drivers lead to poorest performance scenarios. Last, we performed a robustness analysis to identify the most robust emission reduction pathways according to four criteria. Results show that socioeconomic drivers characterized by low economic growth and high inequality lead to highest risk scenarios with poor performance for every objective. The functions projecting heterogeneous impacts lead to higher inequality scenarios. Last, all the robust pathways highlighted the necessity for a fast reduction of greenhouse gases, with most regions achieving carbon neutrality by 2050. Our results suggest that the emission reductions should be implemented taking deeply into consideration the economic inequalities and the responsibilities for historical emissions.

Sommario

Le emissioni antropogeniche di gas serra influenzano il clima a un ritmo senza precedenti e l'aumento della temperatura può portare a numerosi impatti in tutto il mondo. Contrastare il cambiamento climatico richiede urgenti azioni di mitigazione. In questo contesto, gli Integrated Assessment Models sono un utile strumento. Questi modelli collegano aspetti di clima, energia ed economia e sono usati per cercare politiche climatiche ottimali dal punto di vista costi-benefici. Tra questi modelli, RICE50+ ha introdotto una maggiore risoluzione geografica e una migliore considerazione delle disuguaglianze economiche. Questa tesi contribuisce all'analisi delle soluzioni ottimizzate da questo modello (cioè i percorsi ottimali di riduzione delle emissioni). In particolare, abbiamo affrontato l'identificazione di scenari ad alto rischio e di soluzioni robuste. Abbiamo iniziato con la ri-simulazione delle soluzioni su un insieme di scenari futuri plausibili definiti dai più importanti fattori di incertezza del modello: le baseline socioeconomiche, le funzioni di impatto climatico e i casi di emissioni Land-Use. Le performance dei risultati sono state misurate secondo gli obiettivi di welfare, temperatura e disuguaglianza economica. Abbiamo poi applicato un algoritmo di scenario discovery per identificare quali fattori portano a scenari di performance più scarse. Infine, abbiamo eseguito un'analisi di robustezza per identificare i percorsi di riduzione delle emissioni più robusti secondo quattro criteri. I risultati mostrano che i driver socioeconomici caratterizzati da una bassa crescita economica e da un'alta disuguaglianza portano a scenari a più alto rischio con scarse prestazioni per ogni obiettivo. Le funzioni che proiettano impatti eterogenei portano a scenari di disuguaglianza più elevati. Infine, tutti i percorsi robusti hanno evidenziato la necessità di una rapida riduzione dei gas serra con la maggior parte delle regioni che raggiungono zero emissioni nette entro il 2050. I nostri risultati suggeriscono che le riduzioni delle emissioni dovrebbero essere attuate prendendo in considerazione le disuguaglianze economiche e le responsabilità per le emissioni storiche.

Contents

List of Figures

List of Tables

Glossary

B

BAU Buisness As Usual. 24, 25

B

BHM Burke-Hsiang-Miguel. 22, 24, 43, 44, 46, 48, 49, 50, 52, 68, 79, 80

C

CART Classification And Regression Trees. 31, 69

CB Cost-Benefit. 2, 5, 7, 8, 11, 12, 14, 67

CBA Cost-Benefit Analysis. 11, 12, 24, 25, 31, 49, 68, 79

CVaR Conditional Value at Risk. 37

D

DICE Dinamic Integrated Climate-Economy. 2, 7, 8, 12, 14, 20, 21, 22, 23, 24

DJO Dell-Jones-Olken. 24, 43, 44, 46, 48, 49, 52, 68, 79

DM Decision Maker. 13, 14, 34

DP Detailed Process. 2, 7, 8

F

FUND Climate Framework for Uncertainty, Negotiation and Distribution. 7, 12, 20

G

GCAM Global Change Assessment Model. 12

GDP Gross Domestic Product. 16, 21, 23

GHG	Greenhouse Gases. 1, 2, 3, 5, 6, 7, 10, 11, 12, 15, 22, 49, 52, 54, 55, 69
GMT	Global Mean Temperature. 1, 26

I

IAM	Integrated Assessment Models. 2, 4, 5, 6, 7, 8, 9, 10, 11, 12, 14, 15, 16, 17, 20, 67, 69
IPCC	Intergovernmental Panel on Climate Change. 1, 14

L

LDC	Limited Degree of Confidence. 37, 53, 68
LR	long-run. 22, 24, 43, 44, 46, 48, 50, 52, 68, 79, 80
LU	Land-Use. 19, 32

M

MACC	marginal abatement costs curves. 21
MOEA	Multi-Objectives Evolutionary Algorithm. 31

P

PAGE	Policy Analysis of the Greenhouse Effect. 12
PBP	Percentile-Based Peakedness. 36, 39, 53, 68
PBS	Percentile-Based Skewness. 36, 39, 53, 68
PRIM	Patient Rule Induction Method. 3, 4, 19, 27, 28, 30, 31, 32, 33, 49, 50, 67, 68, 69, 79, 80
prstp	rate of social time preference per year. 23

R

R&D	Research and Development. 6, 12
RDM	Robust Decision Making. 14

REMIND REgional Model of Investment and Development. 8, 20

RICE Regional Integrated model of Climate and the Economy. 2, 7, 12, 16, 17

RQ Research Questions. 3, 4

S

SCC Social Cost of Carbon. 10, 11, 12

SR short-run. 22, 24, 43, 44, 46, 48, 49, 52, 68

SSP Shared Socioeconomic Pathways. 3, 4, 9, 19, 21, 24, 31, 41, 42, 43, 44, 46, 48, 49, 50, 67, 68, 69, 79, 80

SWF Social Welfare Function. 17

U

UN United Nations. 1, 15

UNFCCC United Nations Framework Convention on Climate Change. 1

W

WIAGEM World Integrated Assessment General Equilibrium Model. 12

WITCH World Induced Technical Change Hybrid. 12

1

Introduction

Anthropogenic climate change is becoming one of the most important, urgent and challenging issues that humanity has to face. The Intergovernmental Panel on Climate Change (IPCC), the body of the United Nations (UN) with the responsibility of assessing the scientific knowledge on human-induced climate change, regularly releases reports, produced through an immense review of data and compilation of key findings. The recent release of the sixth Assessment Report (*IPCC*, 2021a) emphasized a well-known fact: it is unequivocal that Greenhouse Gases (GHG) emissions from human activities warmed the climate at an unprecedented rate in the last 2000 years (*IPCC*, 2021b).

The increase of the Global Mean Temperature (GMT) affects the whole globe, but with high spatial heterogeneity. Its effects include many observed changes in weather and climate extremes like heatwaves, heavy precipitations and tropical cyclones. Without an immediate and decisive effort to reduce GHG emissions to at least a net-zero level, the rising temperature will exacerbate already present impacts on aspects like human health, economic growth, agriculture (*Carleton and Hsiang*, 2016) up to a risk of mass extinction (*Song et al.*, 2021).

To reduce the GHG emissions, strong climate mitigation policies are needed. In order to be effective, the negotiation and implementation of such policies require strong and effective global cooperation. The United Nations Framework Convention on Climate Change (UNFCCC) has a very important role in establishing international treaties to reduce the human influence on climate change, like the Kyoto Protocol and, more recently, the Paris Agreement (*UNFCCC*, 2015). In particular, the goal of the Paris Agreement is to *hold the increase*

in the global average temperature to well below 2°*C above pre-industrial levels and pursue efforts to limit the temperature increase to* 1.5°*C above pre-industrial levels* (*UNFCCC*, 2015). Despite looking like a very ambitious goal, extensive scientific literature already proved that this agreement represents an economically optimal pathway to mitigate the impacts of climate change, e.g. see *Burke et al.* (2018); *Ueckerdt et al.* (2019); *Hänsel et al.* (2020); *Glanemann et al.* (2020); *Gazzotti et al.* (2021); *van der Wijst et al.* (2021).

As the need for immediate and effective climate policies grows, it is fundamental to develop and implement mitigation and adaptation policies. This is particularly challenging in a context of high uncertainty on the future socio-economic scenarios and climate impacts that will occur. Further complications also arise due to the heterogeneous damages of climate change. In fact, impacts may be unequally distributed between regions: warmer countries, which also tend to be poorer and less responsible for the past GHG emissions, suffer the heaviest climate damages (*Diffenbaugh and Burke*, 2019). These impacts had a relevant influence on economic inequality between countries and, in particularly negative scenarios, such inequalities may start to rise again in the future (*Taconet et al.*, 2020).

A useful instrument used to evaluate, and thus design, climate policies and inform policymakers are the Integrated Assessment Models (IAM). These models, according to *Weyant* (2017), are divided into two main categories: Cost-Benefit (CB) or Detailed Process (DP) IAMs. In particular, CB-IAMs are commonly used for policy optimization. They provide an aggregated representation of climate damages and mitigation costs over a given future climate scenario and optimize a mitigation policy that balances the marginal costs of reducing the GHG emissions and the marginal benefits of the climate policy (*Weyant et al.*, 1995). Optimized policies are often represented by trajectories of GHG emissions that maximize the economic benefit over the scenario considered by the model.

This thesis follows a recent CB-IAM called RICE50+, proposed by *Gazzotti et al.* (2021). RICE50+ is based on the Dinamic Integrated Climate-Economy (DICE) model by *Nordhaus* (2018). DICE is a globally aggregated model that combines a neoclassical model of economic growth with a representation of the climate system and economic damages of climate change to estimate optimal paths for emission reduction. A major limitation of the model is the representation of the world as a single aggregated region. *Nordhaus and Yang* (1996) addressed the issue in a regionalised version of DICE called Regional Integrated model of Climate and the Economy (RICE). However, RICE tackles the issue marginally, representing only 12 regions.

One of the most relevant innovations introduced by RICE50+ is the very high spatial resolution implemented: it considers 57 independent regions. The model provides several optimal solutions, each one representing an optimal climate mitigation policy in terms of GHG emissions reduction. Each solution has been optimized over a plausible future scenario, comprising different socio-economic assumptions and different methods for computing future climate impacts.

1.1 Proposed methodology

In this work, we analyzed the optimal solutions of the RICE50+ model. We generated an ensemble of 60 possible future scenarios, defined on the basis of three relevant uncertain inputs of RICE50+. We then selected five relevant objectives related to welfare, temperature increase due to climate change, and economic inequality. We re-simulated each one of the optimal solutions over the potential scenarios and computed the five objectives.

The output data obtained have been further analyzed using the Patient Rule Induction Method (PRIM) (*Friedman and Fisher*, 1999). This method is a Scenario Discovery algorithm designed to find policy-relevant clusters in the outputs of a simulation model. Lastly, we selected from the scientific literature six well-known robustness metrics that we used to perform a robustness analysis of the solutions of RICE50+. Then, we defined two criteria to select a set of robust solutions. For each chosen solution we analyzed the performance over the objectives and the corresponding emission trajectories across the different regions.

1.2 The research questions

In this work, we aim to answer three major Research Questions (RQ) in order to extend the results obtained by *Gazzotti et al.* (2021).

RQ1

Each solution of the RICE50+ model has been optimized over a specific scenario defined by a combination of parameters of the RICE50+ model, including socio-economic assumptions and climate impacts functions. By re-simulating each solution over the new scenarios we defined and evaluating the objective performances, we aim to investigate how much do the narratives of the Shared Socioeconomic Pathways (SSP)s and climate impact functions affect the RICE50+

optimal outcomes. Therefore, we formulate our first research question as:
RQ1: *To what extent do the drivers of uncertainty (SSPs and climate damages) affect the performance of different objectives for the optimal solutions of the RICE50+ model?*

RQ2

The combination of specific uncertain inputs of the model can define particularly unfavourable scenarios that lead to bad outcomes, like a very high temperature increase or a situation of high inequality. Our second purpose is then to investigate the so-called high-risk scenarios. We want to identify the inputs leading to unsatisfactory outcomes and quantify the importance of the different drivers of the uncertainty of the model in defining such scenarios. Thus, our second research question is:
RQ2: *What are the drivers of poor performance for the objectives examined?*

RQ3

The future possible climate scenarios are characterized by high uncertainty. Therefore, we make use of a robustness analysis in order to identify the most robust solutions of the RICE50+ model, namely solutions that allow us to obtain satisfying outcomes regardless of which future conditions should occur. Our third research question is:
RQ3: *What are the most robust solutions across all the objectives and uncertainties considered? What are their implications for climate policy?*

1.3 Outline of the thesis

The thesis is organized as follows: Chapter 2 reviews the state of the art on the existing types of IAMs and their corresponding use. It includes an overview of the literature on the topic of economic inequality and its representation in IAMs. Chapter 3 presents the RICE50+ model and the methodological procedure followed in this thesis: the generation of the ensemble of scenarios and the re-evaluation of the optimal RICE50+ solutions, the selection of the objectives, the PRIM algorithm and the robustness analysis. In Chapter 4 numerical results and outcomes of the methodology discussed are reported and commented in order to answer each of the research questions. Chapter 5 concludes this thesis summarising the main results, reporting the limitations and discussing future research.

2

State of the art

In this chapter, we describe the state of the art upon which this thesis is based, in order to provide the basic notions necessary for the understanding of this work.

In Section 2.1, we provide an overview on climate policies. In Section 2.2, we introduce the topic of IAMs and their uncertainties, in Section 2.3, we provide insights on the specific class of models CB-IAMs, while in Section 2.5, we present a literature review on the topic of climate change and economic inequality.

2.1 Climate policy

As anthropogenic climate changes acquire importance and unprecedented urgency amongst the global issues that mankind has to face, several instruments to address this challenge are analyzed and proposed by the scientific community. Such instruments usually fall within the category of climate policies. They can be local, national or international and are designed to tackle climate change in two ways. Mitigation policies aim to minimize the extend of climate change, for example by reducing GHG emissions improving energy efficiency, and taxing or regulating GHG emissions and energy sources. Adaptation policies aim to minimize the risks of climate change, for example by erecting safer and more sustainable buildings and infrastructures or restoring damaged ecosystems.

In order to fulfill the temperature target of the Paris Agreement (*UNFCCC*, 2015), more and more ambitious climate policies are needed. Several reviews

of such policies are available in the literature, see *Fischer and Newell* (2008); *Peñasco et al.* (2021). In particular, in a comprehensive review of decarbonization policies, *Peñasco et al.* (2021) provide a framework to assess the impacts of ten different policies. These include building codes and standards, renewable energy obligations, government procurement, public Research and Development (R&D) funding, feed-in tariffs or premiums, energy auctions, energy taxes (like a carbon tax) and tax exemptions, GHG emissions allowance trading schemes, tradable green certificates and white certificates (or energy efficiency standards). Usually more objectives are considered by climate policies, together with climate mitigation and adaptation. Aspects like economic competitiveness and affordability, or fairness and social outcomes are taken into account. This leads to the implementation of policies that could be more popular and effective over more issues, not just the environmental one. The authors, together with the environmental and economics goals, evaluate several additional outcomes related to aspects like technology and innovation or distributional outcomes in order to identify potential trade-offs in the implementation of such policies. While there is wide agreement on the positive outcome of all the policies from an environmental and innovation point of view, other aspects are rather debated. For example, measures like R&D have a positive impact on competitiveness like increasing the probability that a firm receives venture capital fundings (*Howell*, 2017). On the other hand, measures like GHG trading systems and energy taxes may have negative competitiveness and distributional impacts like lowering employment rates because of the higher energy costs (*Scrimgeour et al.*, 2005) and because they may place higher burdens on middle expenditure deciles (*Flues and Thomas*, 2015).

2.2 Integrated Assessment Models

Amongst the many instruments used to evaluate climate policies and inform policymakers, Integrated Assessment Models (IAMs) play a very relevant role and have been used to evaluate climate policies for decades (see *Nordhaus* (1993)). As discussed by *Weyant et al.* (1995) explains, an *integrated assessment* framework combines knowledge from different disciplines in order to explore possible future trajectories of human and natural systems, develop insights about policy effects on efficacy and prioritize research needs. In particular, IAMs connect climate, economy and energy to assess impacts or optimize climate policies.

Two main categories of IAMs are identified by *Weyant* (2017):

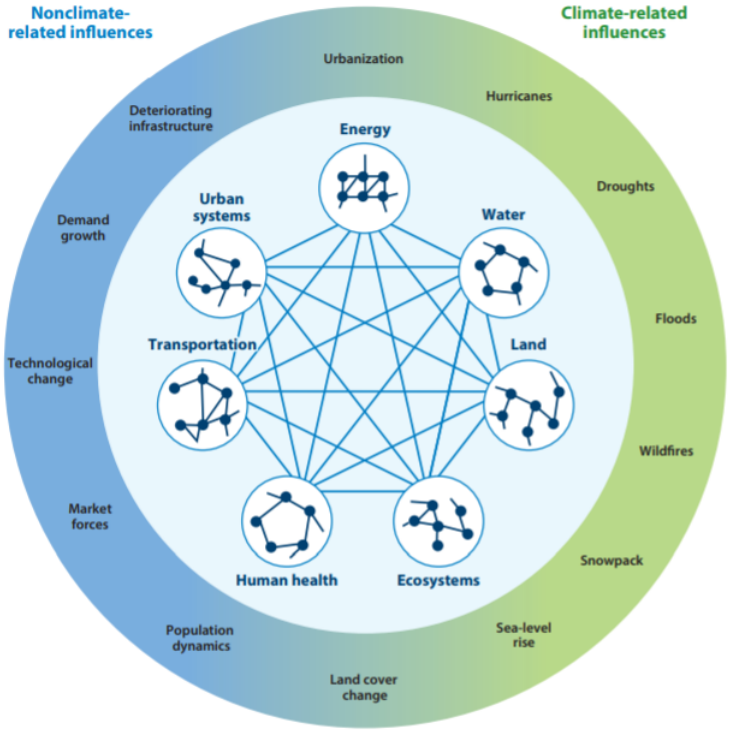

Figure 2.1: *Complex sectoral interactions (Weyant, 2017).*

1. CB-IAMs.
2. DP-IAMs;

Both categories are used to evaluate climate policies, but considering climate impacts differently.

As explained by *Weyant et al.* (1995) and *Fisher-Vanden and Weyant* (2020), CB-IAMs balance the marginal costs of controlling GHG emissions against those of adapting to any climate change and are characterized by an aggregated representation of impact and mitigation costs, usually aggregating sectors and regions into single metrics. Some popular examples of CB-IAMs are DICE (*Nordhaus*, 1993), RICE (*Nordhaus and Yang*, 1996) or Climate Framework for Uncertainty, Negotiation and Distribution (FUND) (*Anthoff*, 2009).

On the other hand, as described by *Weyant* (2017), DP-IAMs are more disaggregated, with their components divided into a number of parts. Their purpose is to provide assessments at a detailed regional and sectoral level. Some models perform this task using detailed economic evaluations of the costs of climate change, others use projections of physical impacts like land inundated by sea level rise or additional heat-stress death. This class of models is typically used to perform mitigation analysis and study the energy-economic impacts on mitigation policies, analyze climate impacts on specific sectors like biodiversity or

water resources. DP-IAMs can also be used to integrate mitigation and impact analysis. This integration is useful because, as countries implement mitigation and adaptation policies, these policies affect the climate. This in turn affects the efficacy of the implemented strategies. These dynamics between the climate and the efficacy of adopted climate policies can be captured and analyzed by DP-IAMs integrating mitigation and impact analysis. Since DP-IAMs provide more information on physical aspects, mitigation costs and impacts on specific sectors, often the results of such models can be used to calibrate the main dynamics of more simple CB-IAMs. Some examples of DP-IAMs are REgional Model of Investment and Development (REMIND) (*Ueckerdt et al.*, 2017, 2019) or IMAGE (*Stehfest et al.*, 2014).

The number of such models has constantly increased up to approximately 20 global scale IAMs (*Fisher-Vanden and Weyant*, 2020). Those model have been developed at different level of complexity, which increased in time, but most importantly depends on the purpose of the IAMs. Usually CB-IAM are more simple, like the original DICE (*Nordhaus*, 1993), which aggregates together the whole world in a single region and uses a Ramsey model of optimal economic growth integrated with a simple representation of the major forces affecting climate change to estimate an optimal path for emission abatement. Those models have a low level of complexity mainly because of the computational effort needed to run them: optimizing a policy using a a highly detailed CB-IAM on time scales of hundreds of years would require an exaggerated amount of time. On the other hand, models like the DP-IAM can have a greatly improved level of detail, like introducing higher degrees of geographical representation and assessments of climate and non-market impacts also on biological and human resources like agricultural impacts and terrestrial and ocean ecosystems (*Reilly et al.*, 2013). Those detailed evaluations are possible because DP-IAM only perform analyses on limited regions and specific aspects of climate change. Figure 2.1 represents an example of the complex interactions between climate and non-climate-related sectors typical of IAMs.

2.2.1 Uncertainty in the Integrated Assessment Models

The use of IAMs includes projecting the future of the world over many decades using several assumptions on aspects like productivity growth, technology diffusion and development and projections about future policies (*Weyant*, 2017). Unsurprisingly, this leads to strong uncertainties. Amongst the most relevant types of uncertainties there are:

1. input uncertainties addressing measurements or the processing operations

like extrapolations;

2. model uncertainties for example in the specification of an aggregate production function;

3. parametric uncertainty such as uncertainties about climate sensitivity.

This can lead to a wide variety of different results between models, for this reason the analyses and understanding of uncertainties in IAMs is of great importance for policymakers. Socio-economic scenarios, climate impact functions (also called damage functions) and climate models outputs are key aspects of IAMs affected by relevant uncertainties. Some frameworks have been proposed to simplify and order all these possible combinations of uncertain factors. For example, the SSP represent a scenario framework based on five narratives describing alternative socio-economic developments, comprising different narratives on aspects like economic and demographic drivers, energy systems, Land-Use change, emissions and mitigation scenarios, depicting a wide uncertainty range on such long term projections (*Riahi et al.*, 2017; *O'Neill et al.*, 2017). The definition of these pathways simplifies the use of all the combinations of socio-economic scenarios, as they represent a universally known point of reference.

Gillingham et al. (2018) use multiple IAMs to provide a detailed exploration of the parametric uncertainty of three parameters relevant for influencing uncertainty in the economics of climate change. The analyzed parameters are: the rate of growth of productivity, the rate of growth of population, and the equilibrium climate sensitivity, defined as the equilibrium change in global mean surface temperature from a doubling of atmospheric CO_2 concentrations. Their aim is to develop a quantification of the uncertainty in policy-relevant model outcomes that are commonly represented in several IAMs, such as: temperature, carbon dioxide concentrations and economic output. Amongst their key findings, the projections of the IAMs are similar when using the modeler's baseline parameters, but diverge when different assumptions on the parameters are used. Despite these differences in the projections, the distributions of the relevant outputs are similar across models with different structures. Lastly, climate-related variables result to have lower uncertainty than economic variables.

Another very relevant source of both uncertainty and debate amongst academics are the climate impact functions. Many functions have been estimated using methods like:

1. expert elicitation, based on interviews with a large number of scientists

to collect their subjective opinion on climate economic impacts (*Nordhaus*, 1994);

2. science-based estimates, imposing physical thresholds like a temperature change that represents a threat to human civilization (*Weitzman*, 2012);
3. econometric methods based on the analysis of economic growth and temperature variation over time (*Dell et al.*, 2012; *Burke et al.*, 2015; *Kahn et al.*, 2019).

Those different approaches lead to a significant uncertainty on the impact estimation, which can span from 0 to -10.2% of GDP for a temperature increases of 1-6°C according to experts elicitation, to an impact of -4.9 to -99% of GDP for temperature increases of 3-12°C according to science-based estimates (*Howard and Sterner*, 2017).

IAMs have been subject of criticism, most relevantly by *Pindyck* (2013, 2017), because of their high uncertainties and, most relevantly, because of how they are designed. Pindyck claims that: *"These models have crucial flaws that make them close to useless as tools for policy analysis"* and give the false impression that we know more than we actually do, thus creating the impression of a scientific legitimacy. The main points of Pindyck critique concern the use of arbitrary parameters, the impact functions, the treatment of uncertainty and the lack of consideration for catastrophic outcomes.

All the impact functions have been criticized by Pindyck, stating that they are made up arbitrarily, without being based on any theory or data. *Pindyck* (2013) claims that the use of these arbitrary functions might not be very relevant for a small temperature increase like 2-3°C since there is consensus that the damages could be small. However, for higher temperature increases such functions would tell us nothing about how much damages to expect.

IAMs also rely on highly uncertain parameters, one of the most relevant being climate sensitivity. According to Pindyck, it is determined by physical mechanisms that are largely unknown ((*Forster et al.*, 2021) for the most recent insights on climate sensitivity).

Trying to treat these uncertainties by assigning probability distributions and running Monte Carlo simulations is not feasible because it is unknown which distributions to assign to the uncertain parameters. Lastly, a problem of IAMs is that they do not take into account catastrophic outcomes, defined as a large decline of human welfare. Even if a similar outcome is highly unlikely, it would be a very relevant driver of the Social Cost of Carbon (SCC). The SCC, defined as the marginal cost of the impacts caused by emitting one extra tonne of GHG, is one of most common climate mitigation policies implemented in IAMs. To

solve these issues and evaluate a SCC, *Pindyck* (2019) proposes a survey of experts giving their opinions on the probability of an extreme outcome of climate change and the reduction of GHG needed to avoid this outcome. Pindyck already considers the input of IAMs as experts' opinions, so a survey would be simpler and transparent.

Lastly, Pindyck also argues that the welfare function upon which IAMs are based is largely dependent from parameters like the index of relative risk aversion and the social time preference. The social time preference, also called discount rate, is an important parameter used in Cost-Benefit Analysis (CBA). It defines a relationship that makes consumptions at different points in time comparable with each other. This is achieved by assigning current values to future consumptions (*Feldstein*, 1964). It reflects society's evaluation of the relative desirability of future consumption: a low value of this parameter favors consumption in future points in time. The value of such parameters, which have a strong influence on the outcomes of the models, is arbitrary and based on ethical arguments. This gives to the modellers a high flexibility to the point that a desired outcome can be obtained by a modeler by simply changing those parameters according to their beliefs.

The social time preference was also at the centre of a debate between William Nordhaus and Nicholas Stern. In his works, Nordhaus usually adopts a rate of social time preference of 3% (*Nordhaus*, 1993). On the other hand, in *Stern* (2006) a value of 0.1% is adopted. Nordhaus argued that the adoption of such a low value is based on ethical judgement, rather than on scientific or economic arguments (*Nordhaus*, 2007a,b). Because of this, *Nordhaus* (2007b) claimed that the conclusions of work proposed by Stern, calling for urgent and immediate action against climate change, were based on results not consistent with the marketplace's real interest rates and savings rates (*Nordhaus*, 2007b). Indeed, Stern provided extensive ethical perspectives on the use of such a low rate of social time preference. The main arguments are reported in *Stern* (2014a) and *Stern* (2014b). However, Stern also asserted that the results of his review were supported not only by ethical judgments but also by updated climate impacts estimate and explicit risk assumptions (*Stern and Taylor*, 2007).

2.3 Cost-Benefit Integrated Assessment Models

This thesis work focuses on the use of CB-IAMs. These models are used to assess optimal mitigation pathways over different scenarios performing a CBA. The CBA accounts for costs and benefits to optimize a policy associated to a given scenario and help a policymaker to choose the most beneficial according

to explicit criteria. From a climate change perspective, a climate policy optimal from a CBA point of view is one for which marginal costs equal marginal benefits. As explained by *Weyant* (2014, 2017), CB-IAMs are widely used mainly for three applications:

1. evaluate optimal trajectories of GHG emissions and the corresponding prices to charge for those emissions;
2. evaluate costs and benefits of non-optimal climate policies;
3. compute the SCC.

An optimal climate policy maximizes welfare value evaluated by the IAM of choice, minimizing the impacts of climate change and the mitigation costs. A policy evaluated by most of CB-IAMs consists in optimizing a control rate on emissions, that can be implemented by imposing a price on the emissions. This corresponds to an optimal carbon tax policy, namely a carbon tax equal to the optimal marginal climate impact and mitigation cost. Other examples of climate policies can be found, for example, in *Chaturvedi and Shukla* (2014). The authors utilize the Global Change Assessment Model (GCAM) to evaluate the energy efficiency role in climate mitigation policies in India and show the importance of energy efficiency in reducing the building sector demand. Further policies like R&D funding to advance technological change and energy efficiency are implemented in such models. For example (*Bosetti et al.*, 2007) implements R&D in the World Induced Technical Change Hybrid (WITCH) model to model technological change induced by climate policy and *Kemfert* (2005) integrates induced technological change in the World Integrated Assessment General Equilibrium Model (WIAGEM), demonstrating both the importance of such feature in the evaluation of mitigation policies and the positive effects of investment projects on energy efficiency.

On the other hand, a non-optimal climate policy consist in a policy pursuing a specified target in terms of, for example, GHG emissions or temperature targets. Such policies are defined as non-optimal because pursuing them result in having higher costs with respect to the optimal ones.

Some of the IAMs most common in the scientific literature, in addition to those already mentioned, are the DICE model (*Nordhaus*, 1993), previously introduced, but also RICE, a regional version of DICE (*Nordhaus and Yang*, 1996), the Policy Analysis of the Greenhouse Effect (PAGE) model (*Nordhaus*, 2007b; *Hope*, 2011) and the FUND model (*Anthoff*, 2009). Notably, updated versions of the DICE model have recently been used to demonstrate that the Paris Climate Agreement represents the optimal policy pathway for this century (*Glanemann*

et al., 2020; *Hänsel et al.*, 2020), result confirmed also by RICE50+ by *Gazzotti et al.* (2021).

2.4 Treatment of uncertainty in Cost-Benefit Integrated Assessment Models

A condition of strict - or deep - uncertainty has been defined by *Knight* (1921) and *French* (1986) as a condition in which it is not possible to say anything at all on the true state of nature: it is neither known nor it is possible to quantify this uncertainty in any way. It is only possible to define a list of possible states of the world. Given the great uncertainty in socioeconomic assumptions, climate impacts and climate scenarios previously mentioned, the analysis of climate policies falls within the discipline of decision making under uncertainty. For this reason it is no longer possible to use approaches based on single best-estimates views of the future (*Lempert et al.*, 2006). These uncertain factors can be explored through the construction and analysis of scenarios (*Giudici et al.*, 2020; *McPhail et al.*, 2020).

In order to evaluate the performances of policies over an ensemble of scenarios, the concept of robustness can be utilized to identify a robust policy. A policy can be defined as so when its performances result to be insensible to changes in future conditions (*Kasprzyk et al.*, 2013; *Maier et al.*, 2016). The evaluation of such policies is useful for policymakers in order to choose between alternatives that can lead to satisfying outcomes regardless of which future scenario should come true. This evaluation task, called robustness analysis, can be performed using a large number of quantitative methods that reflect the level of risk-aversion of a Decision Maker (DM). There are, for example, metrics based on expected value (*Wald*, 1949). Further metrics are based on regret, where regret is defined as the difference between the performance of the selected option for a plausible scenario and the best possible outcome for the same scenario (*Savage*, 1951). Some metrics are based on the satisfaction of a threshold (*Simon*, 1956). Lastly, there are metrics also based on high-order statistical moments (*Voudouris et al.*, 2014; *Kwakkel et al.*, 2016). For a review of proposed methods on describing decisions under uncertainty see *Jonathan et al.* (2015), in which the authors present a taxonomy of robustness frameworks to compare existing different methods to perform robustness analysis based on their methods of alternatives generation, sampling of the states of the world, quantification of robustness measures and identification of key uncertainties using sensitivity analysis.

Robustness analysis represents a very important tool in the analysis of climate policies optimized by CB-IAMs, because it is standard practice to explore the high uncertainties of assumptions and parameters by building large ensembles of scenarios. Simple metrics like Maximin and Maximax (*Wald*, 1949) have been used to evaluate scenarios based on the Fifth Assessment Report of the IPCC (*IPCC*, 2013), and rank climate policies according to the level of risk aversion, showing how the preferences of a DM over uncertainties are as important as the choice of parameters like the discount rate (*Drouet et al.*, 2015). More complex quantitative methods have also been proposed to evaluate alternative climate policies like the Robust Decision Making (RDM) method(*Lempert et al.*, 2006; *Hall et al.*, 2012), which is capable of generating possible robust strategies, represent uncertainties by identifying a plausible set of states of the world and identifies such states where the strategies perform poorly.

2.4.1 Additional climate policy targets in Cost-Benefit Integrated Assessment Models

IAMs are utilized to optimize policies or evaluate specific targets, however this overlooks the fact that climate policies affect a large number of possible stakeholders and can have relevant trade-offs, as previously mentioned. To address this major issue, a recent development in the IAMs landscape has been the introduction of multi-objective analysis to consider additional climate policy targets.

Garner et al. (2016) proposes a version of DICE that considers four objectives: global economic productivity, reliable temperature stabilization, climate damages and abatement costs, quantifying important trade-offs. For example, the authors find a strong disagreement between solutions maximizing global economic productivity and reliable temperature stabilization, and given this disagreement it is unlikely that the two could be formulated as a single objective. Without the use of a multi-objective formulation, this trade-off would have been hidden from policymakers, providing them with a poorer context. A similar analysis has been also proposed by *Marangoni et al.* (2021) using a slightly modified version of the DICE model proposed by *Garner et al.* (2016). The authors uses a multi-objective formulation to analyze adaptive mitigation strategies, which prove themselves to be significantly more convenient, both environmentally and economically, that predetermined strategies, especially in a context of deep uncertainty like climate change.

2.5 Economic inequality

An important aspect of climate change, often overlooked in IAMs, is the spatial heterogeneity of the impacts (*Dell et al.*, 2012; *Burke et al.*, 2015; *Diffenbaugh and Burke*, 2019; *Kahn et al.*, 2019; *Taconet et al.*, 2020) and the economic inequality they lead to.

Three types of economic inequality are distinguished in the literature (*Milanovic*, 2011):

1. unweighted international inequality, which compares countries' GDP per capita by giving the same weight to every country, regardless of their population size;
2. population-weighted international inequality, which weights each country's income by its population, assuming everyone in a country receives the same income;
3. inequality across all individuals in the world.

The second type of inequality, which gives equal weight to every individual, is the most considered in the climate change literature. Growing evidence shows that the impacts on the poors are larger than the impacts on the average population (*Hallegatte and Rozenberg*, 2017), that poor countries will suffer the bulk of the damage (*Mendelsohn et al.*, 2006) and that climate change worsens existing inequalities (*Hallegatte and Rozenberg*, 2017; *King and Harrington*, 2018; *Taconet et al.*, 2020).

Since the wealthiest countries are responsible for the vast majority of historical GHG emissions, the issues of mitigation and adaptation are intertwined with questions of justice on how the mitigation efforts should be shared. The economic damages estimation of the UN mitigation targets (*UNFCCC*, 2015) by *Burke et al.* (2018), based on historical economic responses to temperature variability (*Burke et al.*, 2015), shows that achieving the stringent mitigation target of 1.5°C will likely generate a net global benefit and lessen global inequalities, since the consequences of achieving such target will be unequally distributed with the poorest countries benefiting the most. Such considerations on international justice do not only interest countries, but individuals as well (*Nielsen et al.*, 2021)

Even though some commentators and academics argued that inequality is not an important social problem (e.g. see *Peterson* (2017) for a review of the arguments), a growing scientific literature shows that it is a scientifically interesting question to study the evolution of global inequality and its connections with climate change.

The study by *Diffenbaugh and Burke* (2019) investigates the impact of historical anthropogenic climate change on country-level per capita Gross Domestic Product (GDP), basing their work on previous relationships between economic growth and temperature variability (*Burke et al.*, 2015, 2018). By quantifying the temperature trajectories in absence of anthropogenic forcing in many countries and combining these trajectories with a temperature-GDP response function, the authors calculate the counterfactual per-capita GDP, to calculate the impact of historical forcing on population-weighted country-level inequality. Their results show that warming-induced penalties in poor countries and warming-induced benefits in some rich countries increased inequality between countries to the point that the ratio between the top and bottom population-weighted deciles (*Sala-i Martin*, 2006) over the period 1961 - 2010 is 25% larger than in a world without global warming.

The influence of climate change on within-country inequality would be a critical question, but within-country inequality is difficult to model, requires strong assumptions and comprehensive subnational data on incomes. (*Taconet et al.*, 2020; *Diffenbaugh and Burke*, 2019).

2.5.1 Economic inequality in Integrated Assessment Models and future prospects

Economic inequality is a social issue that has often been overlooked in IAMs, with some notable exceptions. In particular, in their analysis *Taconet et al.* (2020) relies on projections of mitigation costs and climate impacts of multiple IAMs to build country-by-country GDP trajectories up to 2100, exploring 3408 scenarios. Their results show that in scenarios of high climate damages and low mitigation, climate damages may outweigh the forecasted economic catch-up of low-income countries, thus inequalities between countries may stop their declining trend and rise again. *Gazzotti et al.* (2021) also give relevance to economic inequalities, which are introduced in the new welfare formulation of their RICE50+ model. Their results show that even following economically optimal mitigation policies, complying with the Paris Agreement, climate change impacts increase inequalities and this effect can only be partially reduced by mitigation, even in optimistic scenarios of cooperation and care for inequality. Despite the previously mentioned difficulties about data and assumptions, there have also been attempts at representing inequality within geographical regions in IAMs. As a relevant example, *Dennig et al.* (2015) base their analysis on World Bank data on national income and propose a modified version of the RICE by dividing the regions into population quintiles and calculating quintile distributions of income. For their analysis, the authors do not change

the discounting assumptions of Nordhaus (*Nordhaus*, 2007b) and their results show that when climate damages are distributed inversely proportionally to income, the optimal mitigation efforts suggested by their model is equivalent to the optimal mitigation in RICE under the assumptions of the Stern Review (*Stern*, 2006).

In order to improve the evaluation of climate policies with respect to inequality, several options have been suggested. The literature on climate policies traditionally follows a discounted-utilitarian Social Welfare Function (SWF) approach (*Nordhaus*, 1993; *Stern*, 2006), but *Adler et al.* (2017) propose the use of a non-discounted prioritarian SWF, an uncommon approach for the evaluation of climate policies. The concept behind this approach is to give greater weight to well-being changes that affect worse-off individuals and, as the name suggests, the formulation of the SWF following this approach does not include a time-discount factor, thus being impartial between generations. Other practices consist in enhancing the representation of poverty and inequality (*Rao et al.*, 2017), like adopting model features that incorporate social heterogeneity and policy mechanisms. Other dimensions of inequality, currently lacking from the analyses, should be implemented. Quantitative inequalities have been incorporated in IAMs more than qualitative and qualitative inequalities can hardly be summarized by income inequality (*Emmerling and Tavoni*, 2021). For this reason, *Emmerling and Tavoni* (2021) underline the importance of including a more comprehensive list of dimensions of inequality into IAMs, like gender, race and education.

3

Methods

3.1 Introduction

The purpose of this thesis is to analyze how much the narratives of the SSP and impact functions influence the performance of the optimal benefit-cost solutions of the RICE50+ model over an ensemble of possible future scenarios, identify which scenarios have the worst performance, and the importance of the different drivers of uncertainty in defining such scenarios, and performing a robustness analysis to identify the most robust solutions of the model. To achieve these goals, we adopt the methodological procedure illustrated in figure 3.1, which reports the flowchart of the work used to perform the analyses and the results obtained for each one of the three research questions previously introduced in Section 1.2.

To evaluate the performance of the model, we selected relevant objectives in terms of welfare, temperature and economic inequality, and we built an ensemble of possible future scenarios by combining uncertain assumptions of the model such as the SSP, the impact functions and the scenarios of Land-Use (LU) emissions. We analyzed the performances of the optimal solutions of model over their original scenario and over the entire ensemble of scenarios.

We then applied the algorithm of scenario discovery called PRIM (*Friedman and Fisher*, 1999), which is used to identify scenarios that systematically lead to unsatisfying performances and allows to quantify the relevance of every uncertain driver defining those scenarios (*Bryant and Lempert*, 2010).

We implemented six different robustness metrics to perform a robustness

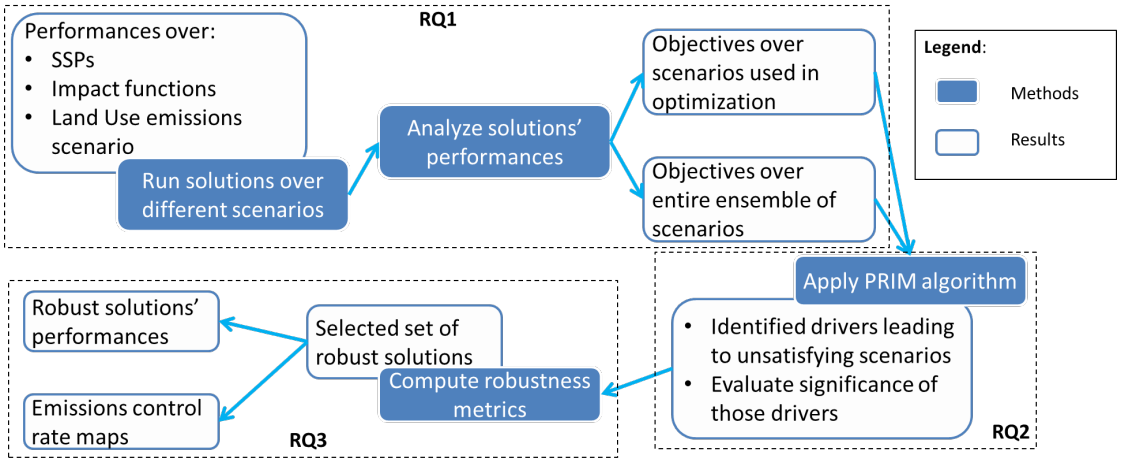

Figure 3.1: *Flow chart of the analysis process. The blue boxes represent the methods applied, while the blue outlines represents the results associated with the methods and the arrows point to the logical progression of the analysis. The chart is divided in three parts by the black dashed lines, associating methods and results to the research question they answe to.*

analysis and analyze the solutions according to those different metrics, covering different risk aversion levels. The results have been used to identify the most robust solutions of the model across the different metrics and objectives, and lastly we analyzed policy-relevant parameters of the most robust solutions like the optimal emission control rate.

In the following sections we explore the different methodologies adopted to perform these analyses.

3.2 The RICE50+ model

This study is based on the benefit-cost assessments of the RICE50+ model by *Gazzotti et al.* (2021), which is based on the DICE model by Nordhaus, specifically the version DICE-2016R2 used in *Nordhaus* (2018). Many IAM have been recently updated to include recent empirical assessments on climate change economic impacts. These include: DICE (*Moore and Diaz*, 2015; *Glanemann et al.*, 2020; *Hänsel et al.*, 2020), REMIND (*Ueckerdt et al.*, 2019) or FUND (*Moore et al.*, 2017). The RICE50+ model also accounts for geographic heterogeneity and inequality as a key component of welfare optimization (*Gazzotti et al.*, 2021). In the following sections, we will provide a brief description of the components of the model that are most relevant for our specific analyses. For more details see *Gazzotti et al.* (2021).

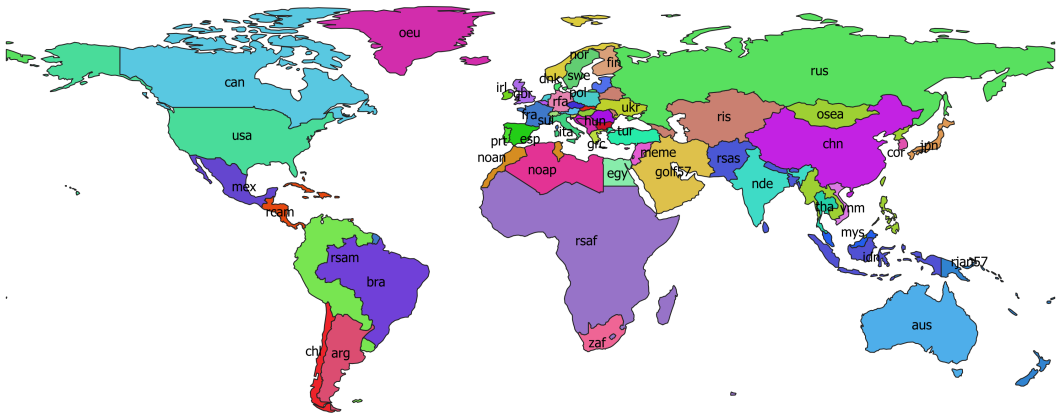

Figure 3.2: *Geographical rapresentation of the regions of the model.*

3.2.1 Regional aggregation and economy

The model accounts for 57 independent regions, based on the finest regional disaggregation of the marginal abatement costs curves (MACC) available. The socio-economic drivers come from the SSP (*Riahi et al.*, 2017). Figure 3.2 shows all the 57 independent regions.

The economic representation in the RICE50+ model is largely based on the representation from Nordhaus DICE model. It computes the GDP production for each region i and time t using a Cobb-Douglas production function:

$$Y_{GROSS,i}(t) = TFP_i(t) \cdot K_i(t)^{\alpha} \cdot L_i(t)^{1-\alpha} \tag{3.1}$$

where $TFP_i(t)$ is the total factor productivity, $K_i(t)$ the capital and $L_i(t)$ the labor. The savings rates $S_i(t)$ determine investments and capital according to:

$$I_i(t) = S_i(t) \cdot Y_i(t) \tag{3.2}$$

and:

$$K_i(t+1) = (1-\delta_k)^{\Delta t} \cdot K_i(t) + \Delta t \cdot I_i(t) \tag{3.3}$$

In DICE they are usually left as free variables to be optimized, but in this case

the savings rates have been fixed starting from historical values and converging linearly to the projections of DICE-2016R2, since the savings were not affecting the results of the optimizations in a meaningful way and were increasing the model complexity.

3.2.2 Emissions abatement

Every region can reduce their GHG emissions by increasing the fraction of emissions to mitigate $\mu_i(t)$, hereafter also called emission control rate. The evolution of this variable is therefore optimized by the cost-benefit analysis. It ranges between $[0, 1.2]$ and, unlike the original DICE formulation, the RICE50+ model also introduces a limitation in the mitigation increasing rate. As *Hänsel et al.* (2020) did, a maximum increase rate of 20% over a 5-years period is fixed.

3.2.3 Climate impact functions

The RICE50+ model implements the following empirically-estimated impact functions:

Burke et al. (2015) impact function

Burke et al. (2015) found a non-linear relationship between economic productivity and annual average temperature, with a maximum productivity at 13 °C and strongly declining at higher temperatures. Using long-run estimates and a single equation for every region, a function of growth effects related to country level temperature was obtained:

$$h(T_i(t) = 0.0127 \cdot T_i(t) - 0.0005 \cdot T_i(t)^2 \tag{3.4}$$

The impact function is hereafter called Burke-Hsiang-Miguel (BHM). The model uses four alternative specifications, which include different time lags, capturing short-run (SR) and long-run (LR) impacts, and accounting for the income differentiation between rich and poor countries. The corresponding specifications are SRdiff and LRdiff.

The impacts on the production growth rate $\delta_{i,BHM}(t)$ are obtained by computing the difference between the result of Equation 3.4 at time t and the same value under *reference temperature* T_{i0}, defined as the average values between 1980 and 2010:

$$\delta_{i,BHM}(t) = h\left(T_i(t)\right) - h\left(T_{i0}\right) \tag{3.5}$$

***Dell et al.* (2012) impact function**

Dell et al. (2012) provide another empirical estimation of a linear relationship between temperature and economic growth. The relationship is composed of a general, almost insignificant in magnitude, effect and a strong negative effect of growth reduction that affects only poor countries, defined as having GDP per capita below the median in the base year. The relationship is formalized as:

$$\begin{aligned}\delta_{i,DJO}(t) = 0.00261 \cdot (T_i(t) - T_{i0}) - 0.01655 \cdot \\ (T_i(t)) - T_{i0}) \mid_{GDPpc_i(t_0) < Median(GDPpc_i(t_0))}\end{aligned} \tag{3.6}$$

***Kahn et al.* (2019) impact function**

The last empirical estimation by *Kahn et al.* (2019) provides an empirical relationship between growth rate and the changes of the country-level temperature over the historical norm. The results show a decrease of growth rate for a one degree both in temperature rising and decreasing. There is no differentiation between rich and poor countries. The relationship is:

$$\begin{aligned}\delta_{i,Kahn}(t) = -0.0586 \cdot \left([T_i(t) - \overline{T}_i(t-1)] - [T_i(t-1) - \overline{T}_i(t-2)]\right) \mid_{T_i(t) > \overline{T}_i(t-1)} \\ -0.0520 \cdot \left([T_i(t) - \overline{T}_i(t-1)] - [T_i(t-1) - \overline{T}_i(t-2)]\right) \mid_{T_i(t) < \overline{T}_i(t-1)}\end{aligned} \tag{3.7}$$

with $\overline{T}_i(t-1) = n^{-1} \sum_{\tau=1}^{n} T_i(t-\tau)$ for $n = 6$.

3.2.4 Welfare

The RICE50+ model implements an extended welfare function with respect to the original DICE. It replicates the idea of maximizing global consumption, but it also allows to gradually change from equal marginal utility to population weighting by using a parameter of inequality aversion γ. It is defined as:

$$W = \sum_{t=1}^{T} \left[\frac{1}{1-\eta} \left(\sum_i w_{pop,i}(t) \left(\frac{C_i(t)}{L_i(t)} \right)^{1-\gamma} \right)^{\frac{1-\eta}{1-\gamma}} - 1 \right] \cdot (1+\rho)^{-t} \tag{3.8}$$

The model uses the four reference levels listed in table 3.1. The parameter ρ represents the utility discount rate, also called rate of social time preference per

γ value	Interpretation
0	No inequality aversion
0.5	Intermediate inequality aversion (default)
1.45	High inequality aversion
2	Very high inequality aversion

Table 3.1: *Inequality aversion alternative values*

year (prstp), and has a default value of 1.5%. The regions can maximize their welfare either in a non-cooperative or cooperative setting.

3.2.5 Land-use

Land-Use (LU) is an exogenous addition to the RICE50+ model dynamics. The model takes the decreasing trend typical of DICE-2016R2 and differentiates two cases: in the first case used for Buisness As Usual (BAU), every region is affected by the decreasing trend. This means that high-emitting countries decrease their emissions over time and countries that start with negative emissions increase their emission towards the zero value. In the second case, used for CBA optimizations, the decreasing trend is applied only to countries that start with a positive value.

3.2.6 The RICE50+ model modification

We modified the RICE50+ model in order to re-simulate its optimal solutions over a range of scenarios. In this new version, the model takes as input the optimal emissions control rate $\mu_i(t)$ of every region over the time period 2020 - 2300, each set corresponding to one of the 479 optimal solutions of the model used in *Gazzotti et al.* (2021).

For the re-simulation of every solution, the model's parameters are set to match the values used to optimize that specific solution. Then, the model re-simulates the solution over an ensemble of 60 scenarios given by the combination of:

1. the five SSPs;
2. the six impact functions described in Section 3.2.3:
    - the four specifications of the BHM function: BHM-SR, BHM-LR, BHM-SRdiff, BHM-LRdiff;
    - the Dell-Jones-Olken (DJO) impact function;
    - the Kahn impact function.

3. the two cases of Land-Use emissions described in Section 3.2.5.

This allows us to explore the uncertainty over climate impacts, socioeconomic and emissions scenarios,

The re-simulations lead to a total of 28.740 model runs, and for each one of them the values of relevant objectives have been extracted. It therefore generates a data set of 28.740 values for each of the five objectives considered (see Section 3.3). Note that inequality aversion and discount rate have not been considered in the generation of the scenarios. For every simulation they are fixed to the values used in the optimization of the corresponding solution.

We performed the analyses on the data set obtained from the model runs and on two other specific subsets:

1. a subset obtained by considering only solutions optimized with the CBA Land-Use emission case, while ignoring the solutions optimized with the BAU Land-Use emission case. This results in 26.940 values for each objective, and hereafter the dataset will be called CBA-subset;

2. a subset obtained by considering only the cooperative solutions resulting in 21.540 data for every objective, here called Coop-subset. Note that the Coop-subset is also a subset of the CBA-subset, since the cooperative solutions have been optimized only considering a CBA Land-Use emissions case.

3.3 Objectives

We carried out the analysis considering relevant objectives in terms of welfare, temperature and economic inequality, all extracted from the runs of the RICE50+ model's solution over the ensemble of scenarios.

3.3.1 Welfare objective

In terms of welfare, the objective that we selected is the welfare value produced by the RICE50+ model, described in Section 3.2.4 up to year 2100. The welfare values have been normalized between 0 and 1 using a min-max feature scaling, so given a set of welfare values W where W_i is the value resulting from scenario i, the normalized welfare value is obtained applying the formula:

$$normW_i = \frac{W_i - min(W)}{max(W) - min(W)} \tag{3.9}$$

The solutions which perform better in terms of welfare will have a value of 1 and the worst a value of 0.

3.3.2 Temperature objectives

As for temperature, the selected objective is the GMT evaluated by the model in the year 2100. The best performances are represented by solutions with the minimum values of temperature increase in 2100.

3.3.3 Inequality objectives

To consider economic inequality, many indices have been proposed in the literature. In this thesis we selected three amongst eight of the most popular (*Sala-i Martin*, 2006).

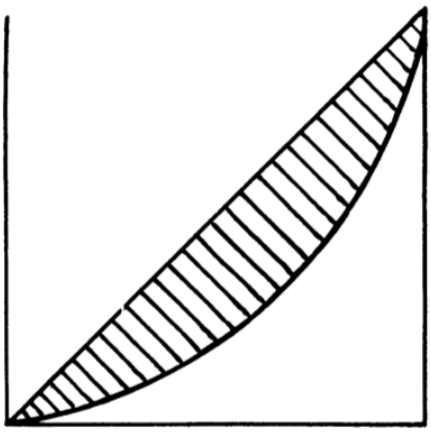

Figure 3.3: *Graphical representation of the Lorenz curve (Gastwirth, 1972).*

The first index that has been selected as objective is the Gini index; this index represents income inequality between a population and it is defined based on the Lorenz curve $L(p)$ represented in Fig.3.3. The curve is defined $\forall p \in [0,1]$ and represents the fraction of the variable measured (like income) that the holders of the smallest p^{th} fraction possess. The Gini index is defined as the ratio of the area between the Lorenz curve L(p) and the 45° line to the area under the 45° line (which is 1/2) (*Gastwirth*, 1972). The Gini index is also commonly defined as half of the relative mean absolute difference. The relative mean absolute difference is the average absolute difference between two individuals or entities in the considered population divided by twice the level of income. Given a population of N entities where x_i is the income of entity i and $\overline{x}$, the Gini index is given by:

$$G = \frac{\sum_{i=1}^{N} \sum_{j=1}^{N} |x_i - x_j|}{2N^2 \overline{x}} \tag{3.10}$$

The second and third indexes selected are the ratios between:

1. top and bottom income deciles (90/10 ratio);
2. top and bottom income quintiles (80/20 ratio);

of the population-weighted country-level per capita GDP (*Sala-i Martin*, 2006; *Diffenbaugh and Burke*, 2019; *Gazzotti et al.*, 2021). According to *Sala-i Martin* (2006):

> *The top-20-percent-to-bottom-20-percent is the ratio of the income of the person located at the top twentieth centile divided by the income of the corresponding person at the bottom twentieth centile. A similar definition applies to the top-10-percent-to-bottom-10-percent ratio.*

The three indexes are referred to the year 2100. The solutions which perform better in terms of economic inequality, meaning that they have minimum levels of inequality, will have minimum values of each of the three selected objectives.

3.4 Patient Rule Induction Method

PRIM, introduced by *Friedman and Fisher* (1999), is a scenario discovery algorithm. Scenario discovery is based on the use of statistical or data mining algorithm to find policy-relevant clusters of cases in large multidimensional datasets of simulation model results. In particular, given a simulation model with inputs $\mathbf{x} = (x_1, x_2, ..., x_n)$ and output y, the purpose of the PRIM algorithm is to determine likely values of y for specified values of $\mathbf{x}$. This algorithm is used to find combinations of constraints on a number of input parameters that predict policy-relevant cases, providing a quantitative justification for the choice of some scenarios with respect to others (*Lempert et al.*, 2008). The algorithm has a wide range of possible applications, from identifying high-risk hospital patients (*Nannings et al.*, 2008), to analyzing terrorism data (*Porter and Brown*, 2007), up to the uncertainty analysis of climate scenarios (*Rozenberg et al.*, 2014; *Taconet et al.*, 2020). In the following section, we will provide a brief description of the algorithm, for more details see *Friedman and Fisher* (1999).

3.4.1 The algorithm

The ultimate goal is to seek a sub-region of the space of input values within which the average value of the output is larger (or smaller) than the average

over the entire input space. It is important to notice that maximizing a function is equivalent to minimizing its negative, so it is possible to consider only the maximization operation. Given a function $f(\mathbf{x})$ with inputs $\mathbf{x}$ and output y, we define S_i as the set of possible values of input x_i, which could represent real or categorical values. The entire input domain S is represented by:

$$S = S_1 \times S_2 \times ... \times S_n \tag{3.11}$$

The goal of the algorithm can be formalized as finding a solution region R, subset of S, so that the average of the input over the R is:

$$\hat{y}_R = \frac{1}{N \cdot \hat{\beta}_R} \sum_{\mathbf{x}_i \in R} y_i \gg \overline{y} \tag{3.12}$$

where $\overline{y}$ is the output average over the entire input space and $\hat{\beta}_R$ represents a property of any sub-region called support and defined as:

$$\hat{\beta}_R = \frac{1}{N} \sum_{\mathbf{x}_i \in R} 1(\mathbf{x}_i \in R) \tag{3.13}$$

The function $1(\mathbf{x}_i \in R)$ is an indicator function that has value of 1 if $\mathbf{x}_i \in R$ and 0 otherwise. Such solution region R is specified by logical conditions involving the values of the input variables, that is, it is defined as the union of a set of K sub-regions $\{B_k\}_1^K$. If s_{ik} represents a subset of possible values of input x_i, then each sub-region B_k, also called box, is defined as:

$$B_k = s_{1k} \times s_{2k} \times ...s_{nk} \tag{3.14}$$

Thus, every box is described by the intersection of subsets of values of each input:

$$\mathbf{x} \in B_k \bigcap_{i=1}^{n} (x_i \in s_{ik}) \tag{3.15}$$

The goal of the optimization procedure is to induce a set of boxes from the data that cover the input space where the output assumes large values. PRIM performs this task in the covering process: the box construction algorithm is applied iteratively to subsets of data, after iteration K the data covered by box B_k are removed and the box B_{k+1} is constructed from the remaining subset. The algorithm iterates until the estimated mean within the boxes or the individual support becomes too small (e.g. below a given threshold).

The box construction procedure is defined patient as it is composed of two steps: a top-down peeling and a bottom-up pasting. The procedure is illus-

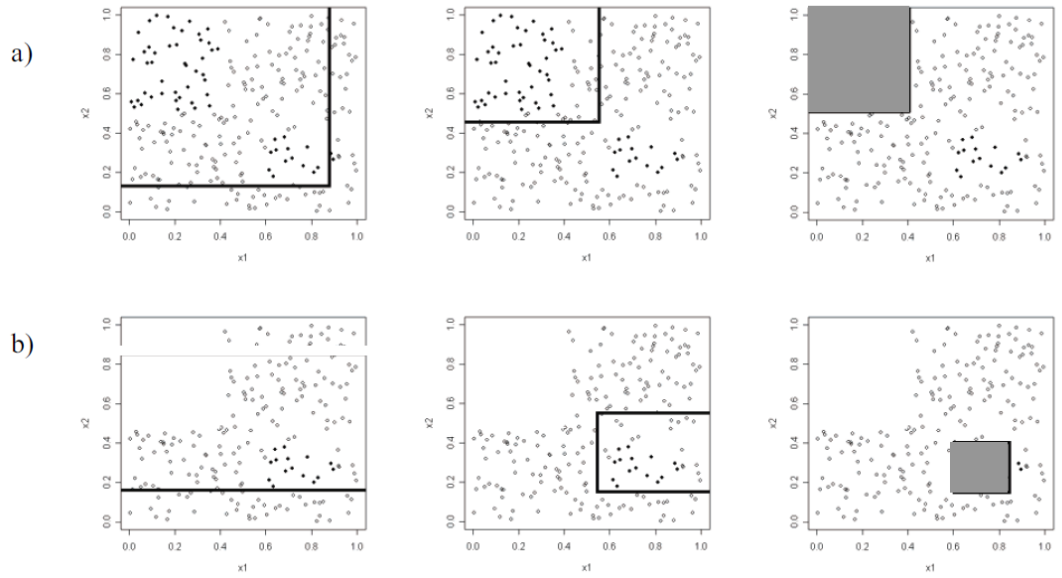

Figure 3.4: *Conceptual illustration of PRIM steps: a) peeling and b) covering process (Lempert et al., 2008).*

trated graphically in figure 3.4.

Top-down peeling

This phase begins with a box B that covers all the data, at each iteration a sub-box b within B is removed. The sub-box b is chosen so that the box resulting from the removal operation has the largest possible output mean value. This peeling procedure stops when the support of the current box β_B becomes smaller than a given threshold β_0, a meta-parameter of the algorithm. Each sub-box eligible for peeling is defined by one input parameter x_i. Inputs that assume real values provide two eligible sub-box that border the upper and lower boundaries of box B on the ith input:

$$\begin{aligned} b_{i-} &= \{\mathbf{x} | x_i < x_{i(\alpha)}\} \\ b_{i+} &= \{\mathbf{x} | x_i > x_{i(1-\alpha)}\} \end{aligned} \tag{3.16}$$

where $x_{i(\alpha)}$ is the α-quantile of the x_i values for data in box B and $x_{i(1-\alpha)}$ the corresponding $(1-\alpha)$-quantile. α is the second meta-parameter of the algorithm. Inputs that assume categorical values provide a set of eligible sub-boxes, one for each of parameter's values in the current box.

Bottom-up pasting

The final box obtained from the peeling procedure has been defined by removing sub-boxes without knowledge of later peels that may have refined even more the boundaries of the box. Therefore, it is possible that the final result may be improved by adjusting some boundaries of the box, through a pasting step. This procedure is the opposite of the peeling step: at each iteration the box B is enlarged by adding a sub-box b so that the box resulting from the adding operation has the largest possible output mean value. The eligible sub-boxes are chosen in the same way as the peeling step. The procedure is iterated until the addition of the next sub-box causes the output mean value to decrease.

3.4.2 PRIM diagnostics

The PRIM algorithm may make several forms of mistakes in performing its task, in particular needlessly slicing off the end of a parameter's range, or including erroneous parameters. For this reason it is important to assess the significance of the parameter's constraints proposed. This can be done using a resampling test or a quasi-p-value test (*Bryant and Lempert*, 2010; *Rozenberg et al.*, 2014).

Quasi-p-value test

This method uses a version of the p-value test to estimate the likelihood that PRIM constrains some parameter by chance. If we consider a single box B_k from the box set B, defined by constraints on parameters in a set S_B, which contains H high value cases amongst a total of T cases, the quasi-p-value is computed considering the box B_{-k}. This box is defined by constraints on all parameter, except one parameter $x_i \in S_B$ amongst the ones defining the box B_k. B_{-k} contains H_{-k} high value cases amongst a total of $T_{-k} \geq T$ cases. The null hypothesis of the test is that the values of interest in box B_{-k} are distributed amongst the T_{-k} values according to a binomial distribution with $p(1) = H_{-k}/T_{-k}$ and the test answer the question: what is the chance that T points drawn from such distribution would have H or more high value cases amongst them? When the ratio H_{-k}/T_{-k} is close to H/T, such chance is high and the contribution of the parameter defining the box B_k is possibly due to chance.

Resampling test

This method evaluates the significance of an input as a driver of the scenario definition by assessing how many times the same input arises from different

samples of the same database. It consists of running the algorithm on multiple sub-samples of the original data set and noting which constraints are consistently considered relevant.

3.4.3 Comparison with other methods

Amongst the algorithm commonly used in the scenario discovery task, PRIM is often compared to Classification And Regression Trees (CART) (*Breiman et al.*, 2017), a classification algorithm (*Lempert et al.*, 2008). CART minimizes misclassification rates to divide the output space into regions of high purity, i.e. regions that contain mainly one output class. The output is given in the form of a decision tree, a hierarchical set of splitting criteria for determining the output class associated with given input combinations (*Lempert et al.*, 2008). The comparison proposed by *Breiman et al.* (2017) finds that both algorithms perform their tasks, but often with imperfections. For example PRIM, as mentioned previously, can restrict too many dimensions and CART may generate too many boxes.

Another comparison that has been proposed by *Kwakkel* (2019) is between PRIM and the Multi-Objectives Evolutionary Algorithm (MOEA) η-NSGAII. While the MOEA gives results that dominate those founds with PRIM, the results are still very similar and the MOEA has the disadvantage of being much more computationally expensive to the point of not recommending its usage instead of PRIM for scenario discovery tasks.

3.4.4 PRIM application

We performed the scenario discovery task by applying the PRIM algorithm, described in Section 3.4.1, to answer to the second research question and evaluate what are the highest risk scenarios and what is the importance of the different drivers of uncertainty. The version that we applied is the Matlab implementation by *Jekabsons* (2015). The PRIM algorithm has been applied to the CBA-subset and the Coop-subset.

3.4.5 Inputs

When applied to the CBA-subset, the algorithm uses as inputs five variables organized in an array where each column corresponds to a variable. Each row, of number equal to the number of data in the subset, is formed by the combination of input values used to obtain the data in the corresponding row of the subset analyzed. The variables are:

1. the five SSP used for the resimulation of the RICE50+ solutions;

2. the six impact functions used for the resimulation of the RICE50+ solutions;
3. the rate of social time preference per year;
4. the inequality aversion;
5. the cooperation level.

Each variable is categorical. When applied to the Coop-subset, the algorithm uses the same input variables, without the cooperation level. The two cases of LU emissions have not been considered as a variable worth investigating because the scenarios defined by the variation of this variable do not have significant differences (see Section 4.2). In both applications, the input arrays have been randomly divided into two equal sets, one for the calibration and one for the validation of PRIM.

3.4.6 Output

As output, the algorithm takes one column of the analyzed subset, corresponding to a given objective. Since there are six objective, PRIM has been applied six different times to each subset, every time considering a different objective as output. The output arrays have also been randomly divided into two equal sets for calibration and validation, coherently with the division of the input arrays. The algorithm implemented by *Jekabsons* (2015) performs a maximization task. Since our purpose was to find the highest risk scenarios corresponding to the worse values of the objectives, we let PRIM search for maximum values while using as objectives the Gini index, temperature in 2100 and both the 90/10 and 80/20 ratios. Since the worse scenarios with respect to welfare have a low value, PRIM in this case should perform a minimization task. To maintain a coherence with the previous applications, we converted the welfare to negative values. This allowed us to find the scenarios with minimum welfare by performing a maximization.

3.4.7 Meta-parameters

The two meta-parameters of the model are α and β_0, mentioned in Section 3.4.1. For α we set a value of 0.05, however every input used is categorical so in this case the value of α has no influence on PRIM. For β_0 we set a value of 0.1, meaning that the box peeling operation continues until the support β of the box (the fraction of data covered by the box, see Equation 3.13) drops below the 10% of the dataset.

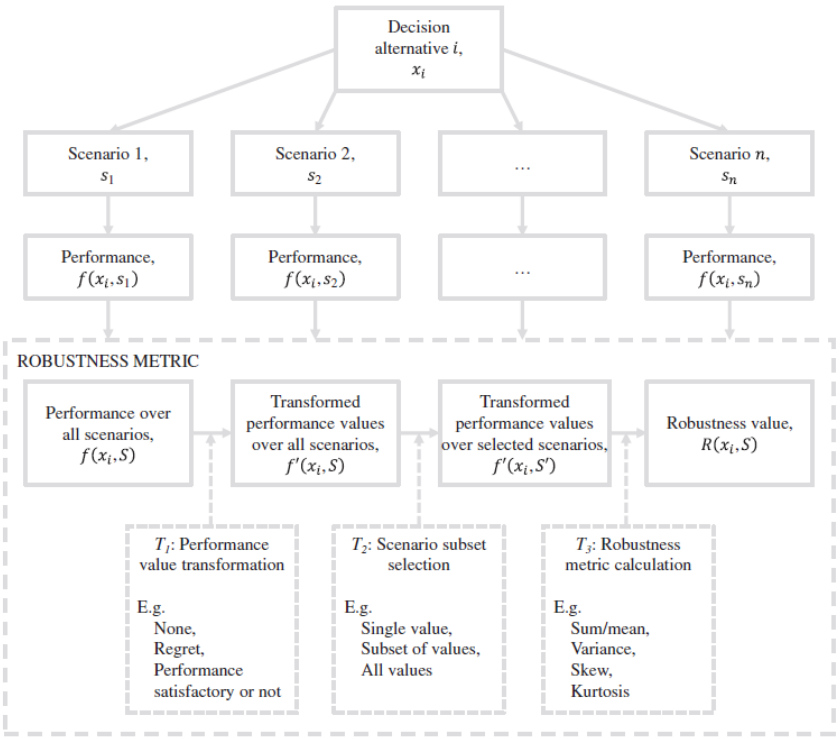

Figure 3.5: *Unifying framework of components and transformations in the calculation of commonly used robustness metrics (McPhail et al., 2018).*

3.4.8 Resampling test

To assess the significance of PRIM results and estimate the importance of the drivers of uncertainty we performed a resampling test: for every application of the algorithm we divided the subset analyzed into 30 sub-samples, run PRIM on every sample and noted which constraints were consistently considered relevant. We considered an input as relevant if it has been considered at least 50% of the times (*Rozenberg et al.*, 2014).

3.5 Robustness analysis

In order to answer to the second research question and identify the most robust solutions of the RICE50+ model over the ensemble of generated scenarios, we performed a robustness analysis evaluating the robustness value of six different metrics which cover a wide range of risk aversion levels. Each metric has been used to evaluate the robustness value of every solution for each one of the five objectives. The work by *McPhail et al.* (2018) provides a useful tool by introducing a framework for the calculation and comparison of a large number of robustness metrics and has been used to select five of the six chosen metrics.

The framework introduced is represented in figure 3.5. Evaluating a robustness metric consists in transforming the performance value $f(x_i, S)$ of an alternative x_i over a set of scenarios S into the robustness value $R(x_i, S)$ of the alternative over the same set of scenarios. Figure 3.5 shows this process broken down into three different transformations: the first, T_1, converts the performance value into the information used in the calculation of robustness. In many cases this is an identity transformation, but some metrics use regret or a constraint to assess whether a performance is satisfactory. The second, T_2, consist in determining which values are used to calculate the robustness, which may be every value, a single one or a subset. The choice of which values to include is a reflection of risk aversion, since the inclusion of more extreme scenarios corresponds to a higher degree of risk aversion. The third transformation, T_3, consists in the actual calculation of the robustness value.

The framework can then be used to decide which metric is appropriate for each decision context. For example, in relation to T_1, the most appropriate metric depends on whether the performance value relates to satisfaction of a constraint or to the optimization of the performances. Regarding T_2, the choice of an appropriate metric depends on the likely impact of system failure and on the risk aversion of the DM. Figure 3.6 shows a classification of robustness metrics commonly used in the literature in terms of relative level of risk aversion from a low level (Maximax, green colour) to a high level (Maximin, blue colour). In relation to T_3, the choice depends on the interest on how the performance values over the different scenarios are summarized (e.g. interest in the average performance of a system vs interest in the variability of the performance of a system over the considered scenarios). It is only applicable to metrics considering more than one scenario.

Such framework proves to be useful, since in the presence of multiple robustness definitions, each one representing different optimistic or pessimistic attitudes of a DM, the definition itself of robustness should be included amongst the uncertainties of the problem, because a misdefinition of the metric capturing the DM's preferences can lead to a degradation of the performances of a system (*Giuliani and Castelletti*, 2016).

3.5.1 Robustness metrics

The metrics we chose will be summarized here. We used the framework by *McPhail et al.* (2018) for the choice of five out of six metrics, in order to select metrics appropriate for the optimization of performance values that could cover a wide spectrum of risk aversion levels. We used such metrics used to

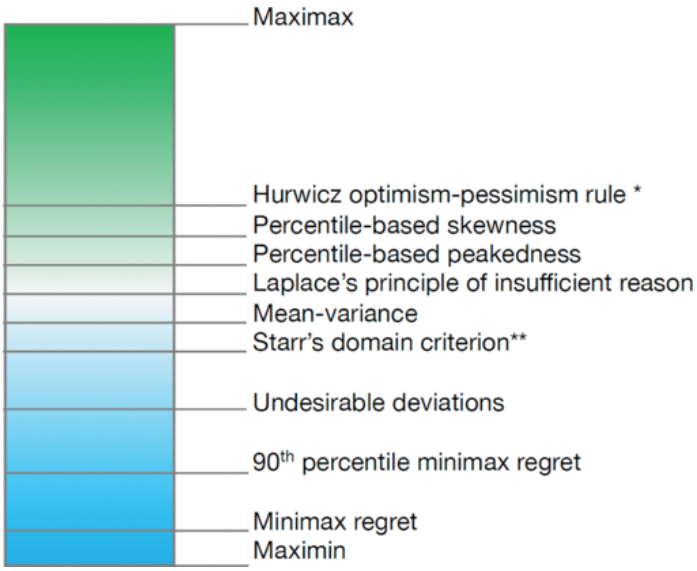

Figure 3.6: *Classification of robustness metrics in terms of relative level of risk aversion from a low level of risk aversion (green) to highly risk averse (blue). Hurwicz optimism-pessimism rule and Starr's domain criterion, because of their formulation, may be placed anywere in the classification (McPhail et al., 2018).*

evaluate the robustness level $R(x_i, S)$ of solution x_i starting from the performance values $f(x_i, s_i)$, where $s_i \in S$ represent the i-th scenario amongst the entire set of scenarios S.

Maximin

The *maximin* metric (*Wald*, 1949) is a metric that represent a very high level of risk aversion, as it focus on the worst possible performance of every solution, also known as security level. It guarantees the selection of a solution that will have a performance at least equal to the security level. The robustness value is:

$$R = arg \max_{x_i} \left(\min_{S} f(x_i, s_i) \right) \tag{3.17}$$

Maximax

The *maximax* metric (*Wald*, 1949) is a metric that represent a very high level of optimism and it is the opposite of the *maximin* metric. It focuses on the best possible performance in a solution. The robustness value is:

$$R = arg \max_{x_i} \left(\max_{S} f(x_i, s_i) \right) \tag{3.18}$$

Mean-variance

The metric *mean-variance* is based on the concept that a robust solution will have a good average result with limited dispersion around it (*Kwakkel et al.*, 2016). It represents an average level of risk aversion. The robustness value is formalized as follows, differentiating between the cases of performances to be maximized or minimized:

$$R = \begin{cases} (\mu_i + 1)/(\delta_i - 1) & maximization \\ (\mu_i + 1)(\delta_i - 1) & minimization \end{cases} \tag{3.19}$$

where μ_i and δ_i are respectively the mean and standard deviation of the performance values $f(x_i, S)$ of solution x_i over the set of scenarios S. The +1 is included to avoid situations where μ_i or δ_i are zero. According to *Kwakkel et al.* (2016), this metric has some downsides: it does not provide insights on the trade-offs between improving μ_i and reducing δ_i, functions combining μ_i and δ_i are not always monotonically increasing and it treats equally positive and negative deviations from the mean.

Percentile-Based Skewness

The metric *Percentile-Based Skewness (PBS)* (*Voudouris et al.*, 2014; *Kwakkel et al.*, 2016) is based on the skewness of the performances' distribution of solution x_i over the scenarios S. It represents an average degree of risk aversion (see Figure 3.6) and the robustness value is:

$$R = \begin{cases} \frac{(f(x_i,s_{90})+(f(x_i,s_{10}))/2-(f(x_i,s_{50})}{(f(x_i,s_{90})-(f(x_i,s_{10}))/2} & maximization \\ -\frac{(f(x_i,s_{90})+(f(x_i,s_{10}))/2-(f(x_i,s_{50})}{(f(x_i,s_{90})-(f(x_i,s_{10}))/2} & minimization \end{cases} \tag{3.20}$$

s_{90}, s_{50} and s_{10} are scenarios that represent respectively the 90^{th}, 50^{th} and 10^{th} percentiles for $f(x_i, S)$. A high value of this metric means that the performance values of a solution are skewed towards better performance values.

Percentile-Based Peakedness

The metric *Percentile-Based Peakedness (PBP)* (*Voudouris et al.*, 2014; *Kwakkel et al.*, 2016) is based on a variation of the kurtosis and represents the peakedness of the performances' distribution of solution x_i over the scenarios S. It represents an average degree of risk aversion, slightly lower than PBS (see Figure 3.6). The robustness value is:

$$R = \frac{f(x_i, s_{90}) - f(x_i, s_{10})}{f(x_i, s_{75}) - f(x_i, s_{25})} \tag{3.21}$$

s_{90}, s_{75}, s_{25} and s_{10} are scenarios that represent respectively the 90^{th}, 75^{th}, 25^{th} and 10^{th} percentiles for $f(x_i, S)$. A high value of this metric implies that the performances value of solution x_i are more peaked around the median value. The version of the metric that we implemented is proposed by *McPhail et al.* (2018) and slightly differs from the version by *Kwakkel et al.* (2016). The latter propose a metric with a double formulation for performances to be maximized or minimized, but this is not needed since this metric assesses the peakedness around the median regardless of whether a performance should be minimized or maximized.

Limited Degree of Confidence

The Limited Degree of Confidence (LDC) (*Aaheim and Froyn*, 2001; *McInerney et al.*, 2012), a metric not discussed by the framework by *McPhail et al.* (2018), is a weighted average between the worst outcome (represented by the maximin criterion) and an expected utility. However, the maximin criterion focuses on the single worst performance of a solution, ignoring other poor outcomes. For this reason, the metric we chose is an alternative formulation proposed by *McInerney et al.* (2012) which replace the maximin criterion with the Conditional Value at Risk (CVaR) (*Pflug*, 2000). This consists in the expected value of the worst q-th portion of the performances distribution of a solution over the scenarios S. The robustness value is then calculated as:

$$R = max \left\{ \beta \left[\frac{1}{N_S} \sum_{i=1}^{N_S} f(x_i, s_i) \right] + (1 - \beta) \left[\frac{1}{qN_S} \sum_{i=1}^{qN_S} f(x_i, s_i) \right] \right\} \tag{3.22}$$

where β is the weight of the weighted average and N_S is the number of scenarios. For the implementation we selected q equal to 0.1, to consider the worst 10-th portion of the performances distribution of every solution and $\beta = [0.2; 0.5; 0.7; 0.9]$.

3.6 Robust solution selection

After evaluating every robustness value, we normalized and ranked the results. The robustness values of each solution x_i over a given scenario $s \in S$ and a given objective O_j, $R(x_i, s)|_{O_j}$, have been normalized between 0 and 1 using a

min-max feature scaling so that the the solution with the best robustness value is associated with a value of 1, in order to allow comparisons between metrics. We ranked independently the robustness values $R(x_i, S)|_{OBJ}$ so that the solution with the best robustness value has the highest ranking, associated with a rank of 1, and the worst a rank of 479. To select the most robust solution $x*$ amongst every x_i according to multiple metrics and across all the objectives, we used two alternative methods.

First method

For every solution x_i we evaluated a function J_i defined as:

$$J_i = \frac{1}{N_{metrics} \cdot N_{OBJ}} \sum_{j=1}^{N_{OBJ}} \sum_{k=1}^{N_{metrics}} (1 - Rank_{j,k})^6 \tag{3.23}$$

This is a function measuring the distance between 1 and the ranking values of solution x_i for every robustness metric over every objective considered. $N_{metrics}$ and N_{OBJ} represent the number of metrics and of objectives respectively. Since the ranking value of 1 represents the best possible robustness value, the robust solution $x*$ will be the one with the minimum value of J_i:

$$x* = min\ J_i \tag{3.24}$$

The power of 6 in the definition of J_i gives more weight to lower rankings.

Second method

The second method is also based on the robustness ranking and consist in the application of what essentially is a maximin criterion, so the robust solution $x*$ will be obtained by:

$$x* = arg\ \max_{x_i} \left(\min_{metrics,OBJ} Rank_{j,k} \right) \tag{3.25}$$

Difference between methods

The first method selects a robust solution that has high robustness ranking across each metric and objective, expressing particular aversion for solutions with specifics bad rankings through the presence of the power of 6 in the formulation. The second method selects a robust solution with a high degree of risk aversion since it focuses on the worst ranking of every solution to select

the one that has the highest worst ranking. The two methods have been selected to highlight solutions with an average robust performance across all the objectives and solutions with the best worst-case respectively.

Application of the methods

The metric PBP is based on the skewness of the performances' distribution of the solutions. The metric PBS, on the other hand, represents the peakedness of the performances' distribution of solutions. Since those two metrics are based solely on the characteristics of the performances' distribution, we decided not to consider them when applying the two methods for the selection of robust solutions previously introduced. Instead, we used PBP and PBS to analyse disagreements between the robust solutions selected by the two methods.

First, we applied the two methods considering the robustness ranking of the four selected metrics for every objective. The aim was to obtain a robust solution representing a compromise between all the metrics and the objectives. Then, we applied the methods to the robustness ranking of the metrics considering only specific objectives. The aim was to obtain a set of solutions, each one robust with respect to an objective. The selected objectives are welfare, the temperature in 2100 and the 90/10 ratio.

4

Results

4.1 RICE50+ optimal outcomes

4.1.1 Experiment setting

To address the first research question formulated in Section 1.2, we re-simulated the 479 optimal solutions of the RICE50+ model over the 60 potential scenarios evaluating the objectives for a total of 28.740 simulations as described in Section 3.2.6 and 3.3. From the resulting dataset we extracted the subset of the cooperative solutions over the same scenarios that were used to optimize them. We analyzed the performances on both this subset and the complete dataset. In the following sections, we will refer to the objective Temperature in 2100 also with the *T2100* notation and to the 90/10 income ratio and 80/20 income ratio with *90/10* and *80/20* respectively.

4.1.2 Results

Performance of solutions in the optimization phase

First, we analyzed the performance of the cooperative solutions with respect to the specific scenario used for their optimization. Figure 4.1 shows these results.

Observing welfare, we notice a clear differentiation between the solutions: the ones optimized using SSP5 lead to the highest values of welfare, followed by solutions with SSP1, SSP2, SSP4 and SSP3. This was expected, since the narratives of SSP5 is characterized by a strong emphasis on economic growth, while SSP1 is a pathway of strong collaboration, technological progress and

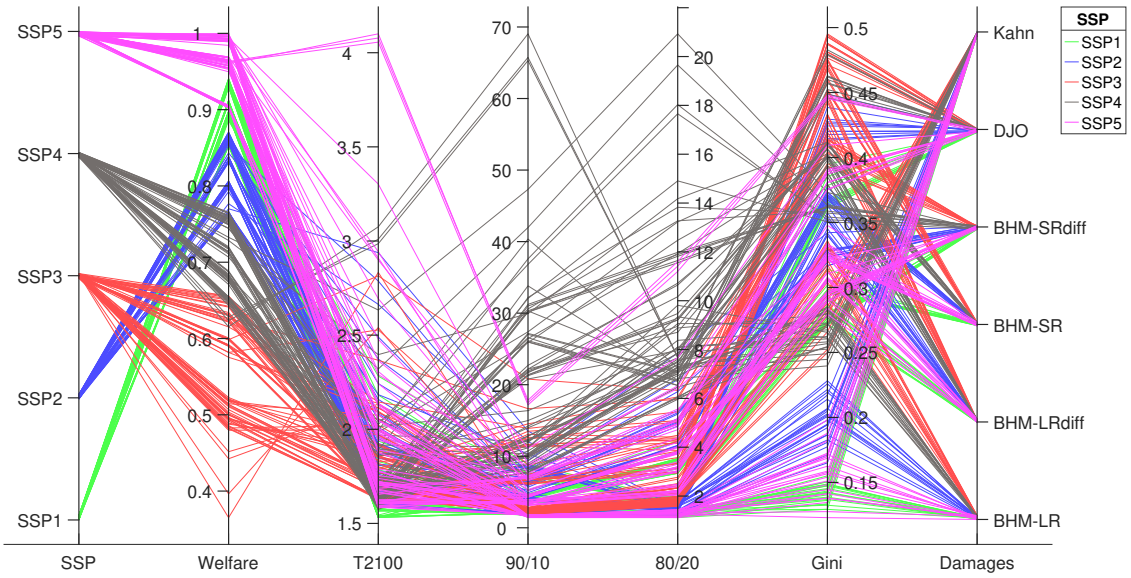

Figure 4.1: *Performances of the optimal cooperative solutions over the objectives: welfare, temperature in 2100, 90/10 ratio, 80/20 ratio and Gini index. The solutions are divided by SSP: green for SSP1, blue for SSP2, red for SSP3, brown for SSP4, magenta for SSP5.*

a shift towards lower resource and energy intensity. On the other hand, SSP4 and especially SSP3 are pathways of slower economic development. See *O'Neill et al.* (2017) and *Riahi et al.* (2017) for a more detailed description on the narratives of the SSPs.

Concerning temperature in 2100, the majority of solutions optimized with SSP1 have lower values than the other solutions, with most of the solutions remaining under 2°C. Solutions designed with the other SSPs lead to temperatures in 2100 which lie between 1.5 - 2.5°C. Considering solutions with temperatures higher than 2.5°C, three of them have been optimized over SSP2 and the others over SSP3-5. These results are also coherent with the narratives of the SSPs since SSP1 is a pathway of sustainability. Consequently, solutions designed over such a pathway reach a low temperature. Differently, the SSP5 is characterized by high exploitation of fossil fuels, SSP4 by investments in carbon-intensive energy sources and SSP3 by strong environmental degradation. Therefore, we expected to find solutions optimized with these SSPs amongst the ones with higher temperatures.

Observing the 90/10 and 80/20 ratios, it emerges that SSP5, SSP1 and SSP2 have the lowest levels of inequality. Solutions with a 90/10 ratio higher than 10 and an 80/20 ratio higher than 6 have been, almost exclusively, optimized over SSP4. The lowest Gini values are from SSP1,SSP 5 and SSP2, while SSP3 and 4 have the highest values, showing concordance between the results for this objective and the 90/10 and 80/20 ratios. These results can be explained by

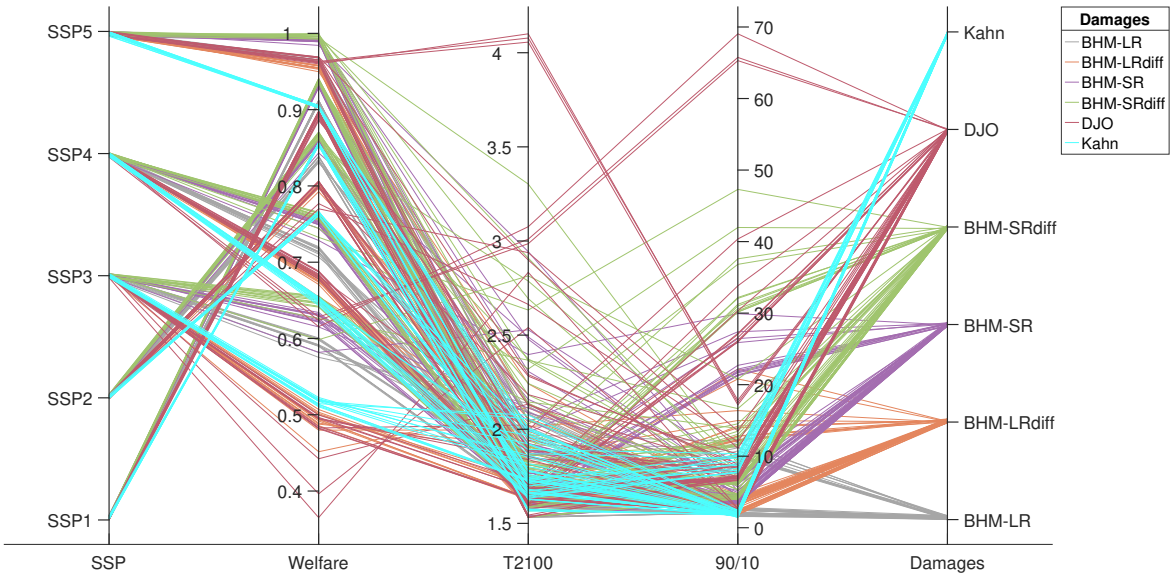

Figure 4.2: *Performances of the optimal cooperative solutions over the three objectives: welfare, temperature in 2100 and 90/10 ratio. The solutions are divided by impact function: grey for BHM-LR, orange for BHM-LRdiff, purple for BHM-SR, green for BHM-SRdiff, bright red for DJO, cyan for Kahn.*

the fact that SSP5 and SSP1 represent pathways of human capital development and inequality reductions, while in SSP2 the inequalities improve slowly. On the contrary, in the SSP3 inequalities persist and SSP4 is a pathway of steadily increasing inequalities between countries.

Since the values of 80/20 ratios and Gini index follow the same behaviour of the 90/10 ratio, their analysis does not provide additional significant information. Hence, in the following sections, we will not furthermore explicitly consider these objectives. Also, we limit our analysis to maintain a coherence with the previous works on economic inequality related to climate change, like *Diffenbaugh and Burke* (2019) and *Gazzotti et al.* (2021).

Figure 4.2 shows the same data as Figure 4.1, but reported by impact function. Observing welfare, we notice that for each SSP, the solutions can be differentiated by impact function. Solutions optimized with BHM-SR and BHM-SRdiff functions have higher welfare values, while the solutions with lower values for every SSP have been designed with BHM-LR and Kahn functions. We can explain these results with the different formulations of the impact functions previously mentioned in Section 3.2.3. These differences lead to contrasting impact projections: BHM-SR, SRdiff and DJO project positive to irrelevant climate impacts on rich regions and damages on poor ones. On the other hand, the Kahn, BHM-LR and LRdiff functions project negative impacts for every region.

Concerning temperature, there is no clear differentiation between solutions with temperature values under 2.5°C. Over that values we find only one solution optimized with the BHM-SR function. The other solutions have been optimized with either DJO or BHM-SRdiff function.

Regarding the 90/10 ratio, the solutions designed with Kahn function, followed by BHM-LR and LRdiff have the lowest values. Solutions with the highest values, like a 90/10 ratio index over 20, have been optimized almost exclusively with DJO, BHM-SRdiff and SR functions. We can explain those results considering that the BHM-SR and BHM-SRdiff functions project positive climate change impacts for rich regions and negative for poor regions. Therefore, they lead to scenarios with a high level of inequality between countries. BHM-LR and Kahn functions project negative impacts for every region, leading to scenarios with lower inequality.

Re-evaluating solutions' performance across all potential scenarios

Having examined the performance of the different solutions with respect to the scenario used in their optimization, we evaluated the performance of the solutions over all potential scenarios by re-simulating them under the six different climate damages impact specifications, the five SSPs and the two cases of Land-Use emissions. The results divided by SSP are represented in Figure 4.3.

The welfare values represented in Figure 4.3a follows a pattern similar to the one showed in Figure 4.1. Solutions re-simulated over scenarios defined by SSP5 and SSP1 have the highest welfare, with a median value of 0.96 and 0.90. SSP2 follows with median welfare of 0.80. Despite the solutions re-evaluated over SSP5 having a higher median and maximum welfare, the ones re-simulated over SSP1 lead to high results with a lower variability, with a minimum value of 0.78 (higher than the minimum value of 0.73 of SSP5). Solutions re-evaluated over SSP4 and SSP3 have the lowest welfare with median values of 0.68 and 0.50, respectively. In particular, SSP3 leads to the minimum welfare values.

The values of temperature in 2100 in Figure 4.3b are lower for solutions re-simulated over SSP1 with a median temperature of 1.76°C. In line with the previous section, solutions re-evaluated over SSP5 have a higher temperature with a median of 2.06°C and a maximum temperature of 4.58°C. Solutions re-simulated over SSP2-4 can also lead to slightly higher temperatures than SSP1.

The 90/10 ratio in Figure 4.3c confirms the pattern highlighted in the previous section, with higher inequalities for solutions re-simulated over SSP3 and

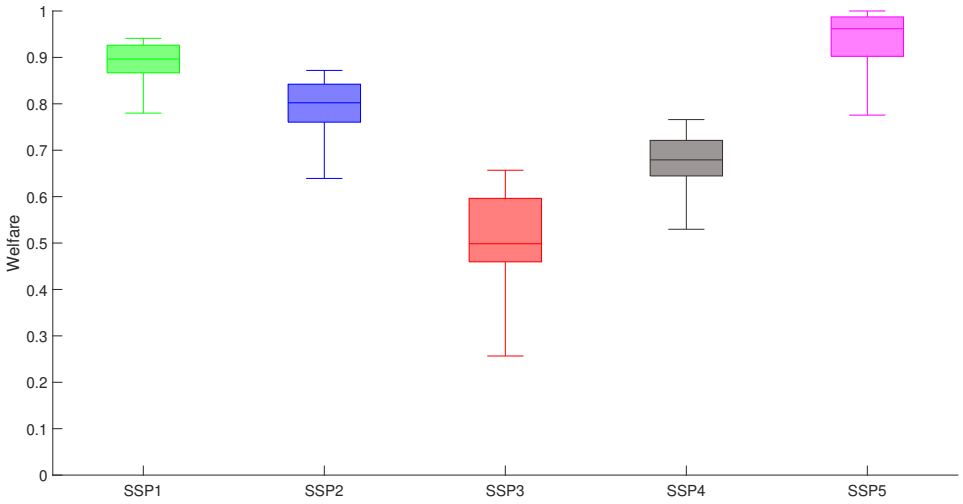

(a) *Welfare*

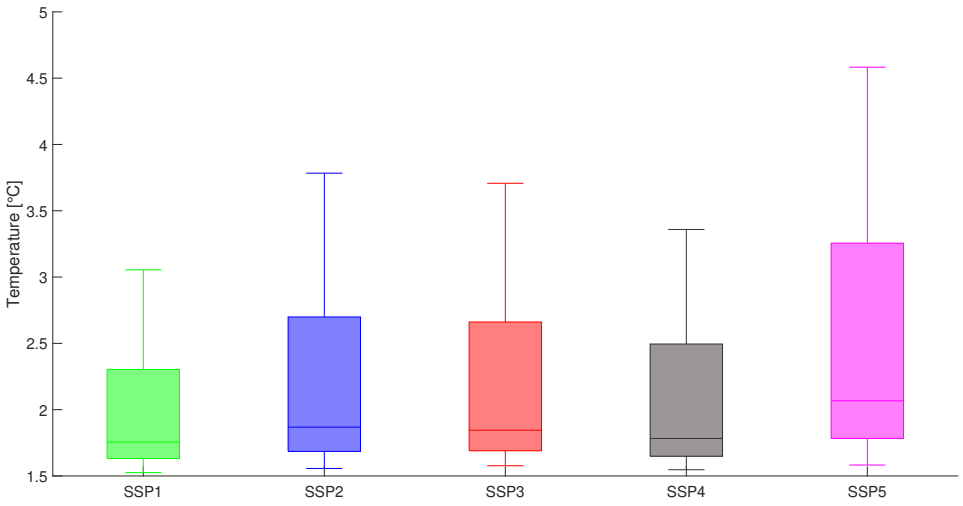

(b) *Temperature in 2100*

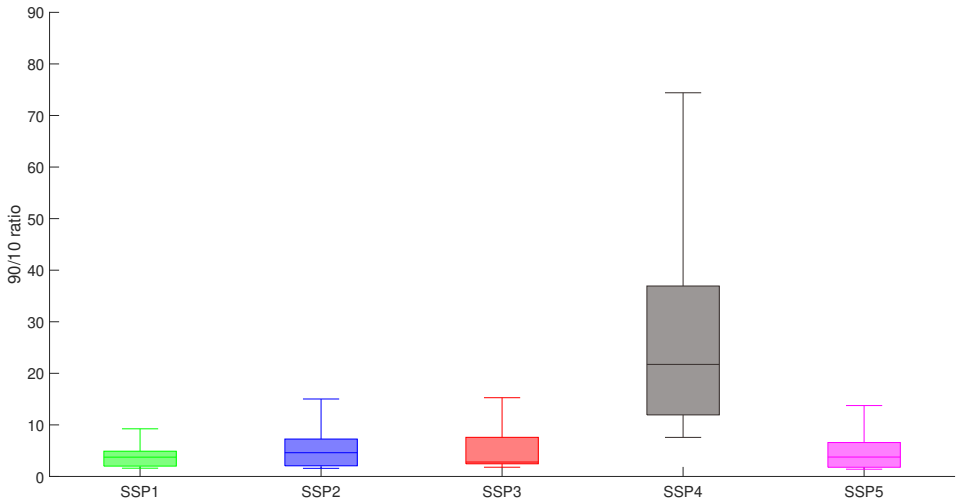

(c) *90/10 ratio*

Figure 4.3: *Performances of the optimal solutions simulated over the entire ensemble of scenarios. (a) represents the welfare values, (b) the temperature in 2100, (c) the 90/10 ratio. The solutions are divided and colored by SSP: green for SSP1, blue for SSP2, red for SSP3, brown for SSP4, magenta for SSP5.*

4, the pathways of strong inequality. In particular, SSP4 leads to the highest values of the 90/10 ratio with a median of 21.73 and a maximum value of 85.26.

Figure 4.4 represents the same data of Figure 4.3, but reported and coloured by damage function specification. The temperature values in Figure 4.4b do not show relevant differences between the different damage functions. We find slight differences in the welfare values represented in Figure 4.4a. These values are higher for the solutions re-simulated over the functions BHM-SR and SRdiff, which both have median values of 0.86. However, observing the values of the 90/10 ratio in Figure 4.4b, we notice that the solutions re-evaluated over those functions lead to higher economic inequality. The solutions re-simulated over the DJO function have lower welfare values than the previous two functions but lead to even higher values of 90/10 ratio index.

Specifically, the solutions simulated over the BHM-SR function have a median value of the 90/10 ratio of 6.03 and in scenarios of very high inequality, they can reach a value of 40.05. We notice even higher values for the SRdiff function, with a median of 9.58 and a maximum of 69.25. The solutions re-simulated over the DJO have a median value of 8.63, but they show greater variability and have the highest maximum values of the 90/10 ratio.

We find the lowest welfare values associated to solutions re-simulated over the functions Kahn (with median welfare of 0.75), BHM-LRdiff (with a median

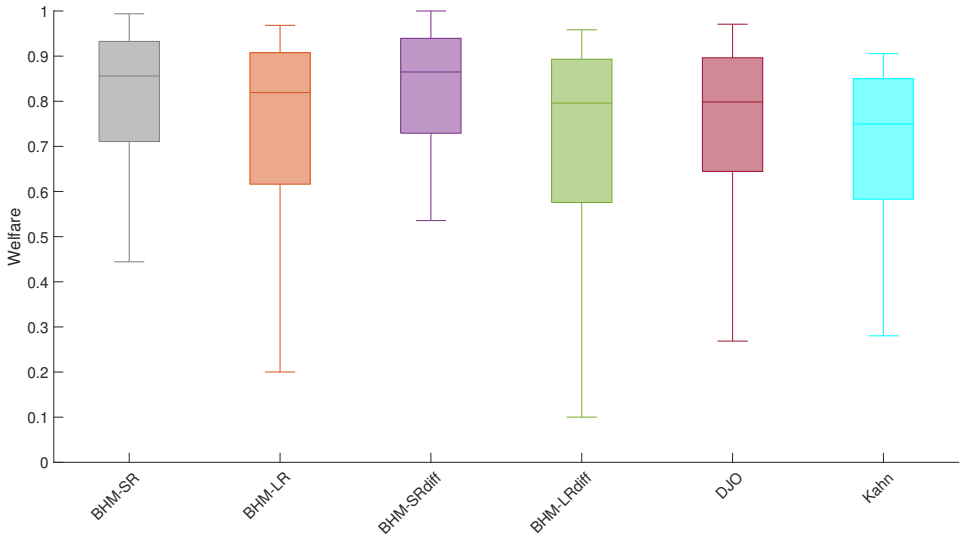

(a) *Welfare*

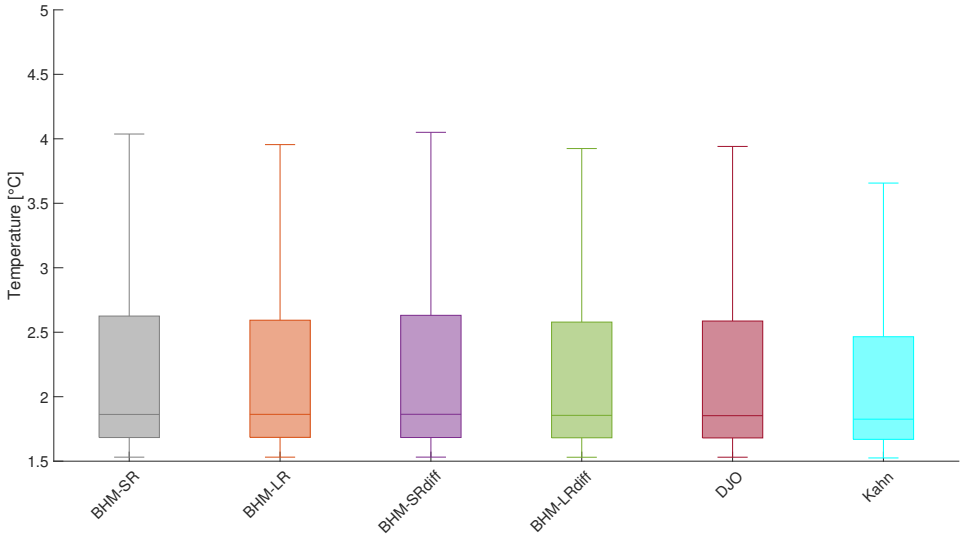

(b) *Temperature in 2100*

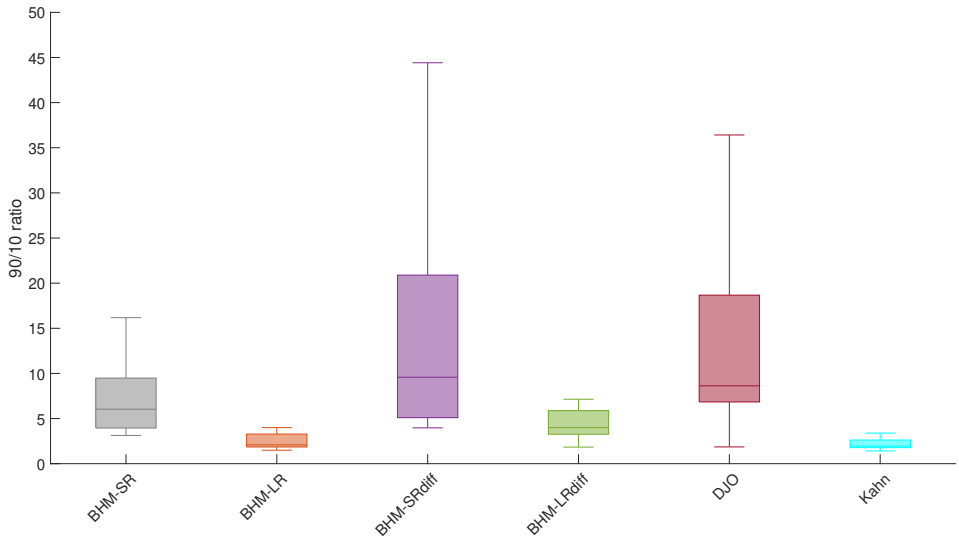

(c) *90/10 ratio*

Figure 4.4: *Performances of the optimal solutions simulated over the entire ensemble of scenarios. (a) represents the welfare values, (b) the temperature in 2100, (c) the 90/10 ratio. The solutions are divided and colored by damage function: grey for BHM-LR, orange for BHM-LRdiff, purple for BHM-SR, green for BHM-SRdiff, bright red for DJO, cyan for Kahn.*

of 0.80) and BHM-LR (with a median of 0.82). According to the values of the 90/10 ratio, these functions are also associated with the lowest economic inequality. The median values are lower than 4, and only a few scenarios with the BHM-LRdiff function lead to a 90/10 ratio higher than 20.

We can explain these results with the different formulations of the impact functions previously mentioned. The Kahn, BHM-LR and LRdiff functions project negative impacts which are more homogeneous across regions than the other functions. Rich and poor regions both suffer damages, and this can lead to scenarios with lower welfare values and lower inequalities across countries. On the contrary, as previously mentioned, the functions BHM-SR, SRdiff project benefits for the rich regions as a consequence of climate change. The DJO function projects a negligible effect on rich regions and impacts on poor ones. Threfore, the differentiation between rich and poor can lead to scenarios where few rich regions improve their welfare, thus leading to the high welfare values represented in the results. However, the poor regions suffer high climate impacts. This differentiation can explain the high values of the 90/10 ratio.

The results show that the narratives of the SSPs and the damage functions affect significantly the outcomes of the optimal solutions of the RICE50+ model. Additionally, they show that scenarios that seem to lead to satisfying welfare values can also lead to high economic inequality between rich and poor regions,

as is the case for solutions re-simulated over the functions BHM-SR, SRdiff and DJO and pathways of high inequality like SSP3 and SSP4. These scenarios raise ethical concerns and questions of international justice. The richest countries, responsible for the majority of the past GHG emissions, can significantly increase their welfare, while the poorest and less liable countries suffer the highest damages. Together with justice issues, these results also raise policy-relevant concerns. In scenarios of high economic inequality, the worse-off countries may also suffer serious consequences in terms of social and political aspects like immigration and political instability (*Barnett*, 2003; *Carleton and Hsiang*, 2016; *Sofuoğlu and Ay*, 2020).

4.2 Highest risk scenarios

4.2.1 Experiment setting

We here consider the second research question of the thesis introduced in Section 1.2. In this second experiment, we wanted to identify the highest risk scenarios in terms of low welfare, as well as high temperature values and high economic inequality. Secondly, we wanted to quantify the importance of the different drivers of uncertainty in defining the high risk scenarios. To perform this task, we applied the PRIM algorithm and we executed a resampling test as described in Section 3.4.1 and 3.4.4. We performed the analysis on two subsets. The first CBA-subset considers only the values obtained by the simulation of solutions optimized with the CBA Land-Use emission setting, supposing decreasing or constant land use emissions. The second is the Coop-subset, with the values obtained by the re-simulation of solutions optimized with the cooperative setting. In the following Section, we report the results of the analysis of the cooperative solutions. The results of the first analysis are reported in the Additional Material, in Section A.1.

4.2.2 Results

Analysis of cooperative solutions

Cooperation is by far the most important driver for high-risk scenarios for every objective considered, as reported in Section A.1. To focus better on the other drivers of uncertainty, we decided to remove the non-cooperative solutions and apply the PRIM algorithm to the Coop-subset only. As explained in Section 3.2.6, the dataset is obtained considering only the values obtained by

the re-simulation over the 60 scenarios of solutions optimized with the cooperative setting.

We reported the results graphically in a similar way as *Kwakkel and Jaxa-Rozen* (2016): the input of PRIM are on the columns, the boxes identified by the algorithm are on the rows. On each row, the red cells represent the rules of the box. Mean and support are in the last two column, while the results of the resampling test are in the last row. As stated in the previous Section, we did not consider the objectives 80/20 ratio and Gini index, because their analysis did not provide additional meaningful information.

In Figure 4.5 we represented the results on the validation set for welfare, temperature in 2100 and 90/10 ratio.

By applying PRIM to the welfare objective represented in Figure 4.5a, we identified four boxes with an average value lower than the global average of 0.78. The boxes cover 10% of the dataset each. The results are coherent with the ones represented in Figure A.1a: the significant inputs are the SSPs, the damage functions and the inequality aversion. The SSP3 and SSP4 are still the relevant drivers for low welfare scenarios due to their narrative of low economic growth. The most relevant damage functions are BHM-LRdiff and Kahn. As in the previous Section, the selected functions are the ones that project damages to every region. In this case, the algorithm selected every inequality aversion level. However, the most relevant is the value 0, representing no inequality aversion.

The analysis of temperature in 2100 produced four boxes with an average lower than the global average. As represented in Figure 4.5b, they cover from 10% to 11% of the data. All the inputs are significant, and the selected values are not very different from the results displayed in Figure A.1b. In this case, the algorithm selected all the SSPs and inequality aversion values. However, the most relevant values remain the SSP2, SSP3 and SSP4, as well as the 0 and 0.5 values of inequality aversion.

In Figure 4.5c we represented the results of the PRIM application on the 90/10 ratio. We displayed three boxes covering from 10% to 14% of the data. The significant inputs are the SSPs and the damage functions. The results are not significantly different from the previous analysis of the same objective.

Considering the results of the two cases analyzed, we can conclude that the SSPs are significant drivers of high-risk scenarios for each objective. Specifically, SSP3 for every objective, SSP2 and SSP5 for temperature, SSP4 for welfare and inequality. SSP1 is the pathway that does not lead to high-risk scenarios in any objective. It highlights the need for policies for sustainable economic and technological development, applied with efficient cooperation.

	SSP					Damage function						Prstp			Inequality aversion				Mean	Support
	SSP1	SSP2	SSP3	SSP4	SSP5	BHM-SR	BHM-LR	BHM-SRdiff	BHM-LRdiff	DJO	Kahn	0.001	0.015	0.03	0	0.5	1.45	2	0.78	10770
Box 1			■				■		■	■	■				■		■	■	0.50	0.10
Box 2			■	■					■	■	■				■	■		■	0.61	0.10
Box 3			■	■		■	■		■		■				■	■	■		0.67	0.10
Box 4			■	■															0.70	0.10
Leftovers																			0.90	0.60
Significance	100%					100%						26.7%			60%					

(a) *Welfare*

	SSP					Damage function						Prstp			Inequality aversion				Mean	Support
	SSP1	SSP2	SSP3	SSP4	SSP5	BHM-SR	BHM-LR	BHM-SRdiff	BHM-LRdiff	DJO	Kahn	0.001	0.015	0.03	0	0.5	1.45	2	1.86	10770
Box 1		■	■		■									■	■	■			2.36	0.10
Box 2		■	■	■	■									■	■	■	■		1.98	0.10
Box 3	■	■	■		■									■	■	■		■	1.92	0.10
Box 4		■	■	■	■	■	■	■	■	■			■	■	■	■			1.97	0.11
Leftovers																			1.72	0.59
Significance	100%					86.7%						100%			100%					

(b) *Temperature in 2100*

	SSP					Damage function						Prstp			Inequality aversion				Mean	Support
	SSP1	SSP2	SSP3	SSP4	SSP5	BHM-SR	BHM-LR	BHM-SRdiff	BHM-LRdiff	DJO	Kahn	0.001	0.015	0.03	0	0.5	1.45	2	8.46	10770
Box 1				■		■		■		■									34.26	0.10
Box 2				■															12.75	0.10
Box 3		■	■	■				■		■									8.19	0.14
Leftovers																			3.72	0.67
Significance	100%					100%						10%			20%					

(c) *90/10 ratio*

Figure 4.5: *Results of the PRIM analysis on: (a) welfare, (b) temperature in 2100, (c) 90/10 ratio, considering only the dataset obtained by the simulation of the cooperative solutions. On the columns there are the inputs, on the rows the boxes. The red cells represent the rules of the boxes. In the last two columns there are mean and support of each box. The results of the resampling test are in the last row expressed as significance.*

Impact functions are also significant drivers of high-risk scenarios for each objective. In particular, the Kahn, BHM-LRdiff and LR functions lead to low welfare scenarios. On the other hand, BHM-SRdiff and SR lead to scenarios with high economic inequality. The DJO function is relevant for both objectives: it projects just a negligible effect on the rich regions, and because of the damages on the poor regions, the function is a driver for low welfare scenarios. At the same time, due to its differentiation, it also leads to scenarios with high 90/10 ratios.

These results highlight the importance of economic inequality as a policy-relevant issue. The occurrence of such diversified damages suggests taking into consideration policies to reduce economic inequality. In scenarios of benefits for the wealthiest regions and impacts for the worse-off ones, it could be convenient to consider redistribution objectives when designing climate policies. Moreover, according to the results, the regions that are wealthier and more responsible for the historical GHG emissions should consider sustaining the major mitigation efforts.

Finally, from the results of welfare and temperature, we can conclude that inequality aversion and the rate of social time preference are significant drivers of high-risk scenarios. A scenario discovery analysis considering a higher number of scenarios defined also by the combination of those two inputs may be an interesting future development.

4.3 Robust solutions

4.3.1 Experiment settings

To answer the third research question we posed in Section 1.2, we evaluated the robustness value of every solution over the five objectives. For every objective, we used the robustness metrics introduced in Section 3.5.1. We based the analysis on the complete dataset obtained by the re-simulation of every solution of the RICE50+ model over the 60 scenarios. Then, using the methods introduced in Section 3.6, we selected four representative robust solutions. We analyzed the performance of the chosen solutions and assessed their emission control rate (also called μ).

Solution	PBP	PBS
W1	0.59	0.27
W2	0.67	0.23

Table 4.1: *Robustness values of the solutions W1 and W2 according to the PBP and PBS metrics.*

4.3.2 Results

Robust solutions selection

First, we evaluated the robustness values for every solution. Then, we proceeded by removing the dominated solutions and focusing the analysis on the non-dominated ones. A solution s_i is defined as non-dominated when there is not any other solution $s_j \in S$ whose robustness values are all higher or equal to the values of s_i.

After that, we applied the selection methods to the non-dominated solutions. First, as explained in Section 3.6, we considered the rankings of the robustness metrics maximax, maximin, mean-variance and LDC (all four specifications) for each objective. By doing this, we selected a compromise solution with high robustness across every objective. Second, we considered the three most relevant objectives: welfare, the temperature in 2100 and the 90/10 ratio index. We repeated the selection procedure three times, each time considering one of these objectives independently. For each selection procedure, we chose one solution for a total of three solutions, which resulted in being the most robust for the three objectives, respectively.

In every application the two methods agreed in selecting the same robust solutions, except for the case of welfare. When selecting the robust solution considering only the metrics evaluated over welfare, we obtained two different solutions, here called *W1* and *W2*. To select a single robust solution between the two, we analyzed the robustness using the metrics PBP and PBS, whose values are reported in Table 4.1.

The two metrics show a trade-off between the solutions. *W1* has higher robustness according to PBP. This means that the performances of this solution are more peaked around the median value. On the other hand, *W2* is more robust according to PBS. This reflects the fact that the performances of *W2* are more skewed towards better values. Neither the two methods for the robust solution selection nor the analysis of the additional metrics can point to the most robust solution. For this reason, we decided arbitrarily to focus the analysis on the solution called *W1*. In the following sections, we will refer to it as *Welfare solution*.

In Table 4.2 we reported the four robust solutions we selected and the values

Solution name	SSP	Damage function	prstp	Inequality aversion	Cooperation level
Compromise	SSP3	DJO	0.015	1.45	coop
Welfare	SSP5	DJO	0.03	1.45	coop
Temperature	SSP1	BHM-LR	0.001	0	coop
90/10	SSP3	DJO	0.03	2	coop

Table 4.2: *Set of selected robust solutions and values of the parameters of RICE50+ used to optimize each solution.*

of the RICE50+ parameters used to optimize each solution. In the first row of the table we reported the name we will use in the following sections to refer to each solution. We chose the names according to the objectives we considered when selecting each solution, so:

1. **Compromise solution**: selected considering the robustness metrics evaluated over every objective;
2. **Welfare solution**: selected considering the robustness metrics evaluated over the welfare objective;
3. **Temperature solution**: selected considering the robustness metrics evaluated over the temperature in 2100 objective;
4. **90/10 solution**: selected considering the robustness metrics evaluated over the 90/10 ratio objective.

Performance of the robust solutions

In Figure 4.6 we represented the performances of the four robust solutions over the 60 scenarios.

In terms of welfare, the Welfare solution leads to the highest minimum scenarios compared to the other solutions. On the other hand, the Compromise solution and the Temperature solution lead to the worst cases. Regarding the temperature in 2100, the best scenarios belong to the Temperature and Compromise solutions. The 90/10 solution leads to scenarios with higher temperatures. In any case, considering every solution, few scenarios go beyond 2°C. Considering the 90/10 ratio, we notice that all solutions lead to scenarios with low values, however, there are still many scenarios with high economic inequalities.

Emission control rate map

Lastly, we analyzed and reported the emission control rate of every solution we selected. This allowed us to describe the most robust GHG emission reduction

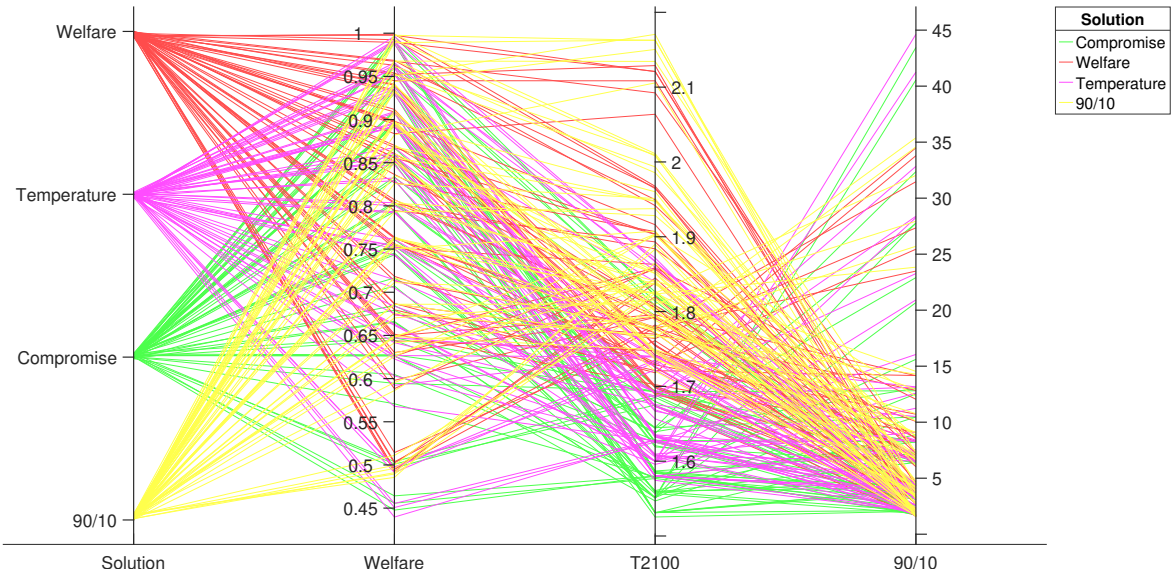

Figure 4.6: *Performance of the selected robust solutions over the 60 scenarios for the objectives welfare, temperature in 2100 and 90/10 ratio. The solutions are divided by colour: green for the Compromise solution, red for the Welfare solution, purple for the Temperature solution and yellow for the 90/10 solution.*

policies that have been optimized by the RICE50+ model. For every solution, we reported the emission control rate in maps for four representative years: 2030, 2050, 2080 and 2100. The complete data sets used to produce the maps are reported in the Additional material, in Section A.2.

We reported the emission control rates of the Compromise solution in Figure 4.7 and 4.8. In the year 2030, represented in Figure 4.7a, every region has an emission control rate of 43%. This result is obtained from an initial emission control rate of 3% in 2020. Then, as explained in Section 3.2.2, the maximum increase of the emission control rate is 20% every 5 years. In 2050, 42 regions out of 57 reach an emission control rate of 100%, thus reaching net-zero emissions. The emission reduction of these regions goes over 100% in 2080, as represented in Figure 4.8a. This means that those regions have negative GHG emissions. After that, the control rate does not change significantly from 2080 to 2100. On the other hand, the emissions control rate of the remaining regions lies between 69 - 98% in 2050. These values increase slightly in 2080 and 2100, but without reaching 100%. We can notice that the regions with a lower emission control rate are Sub-Saharan Africa, the regions of the Middle East and Central America. These regions lie around the tropical area and tend to be poorer than the ones in the temperate area. Therefore, requiring a lower mitigation effort from these regions is coherent with a climate policy that considers economic inequalities.

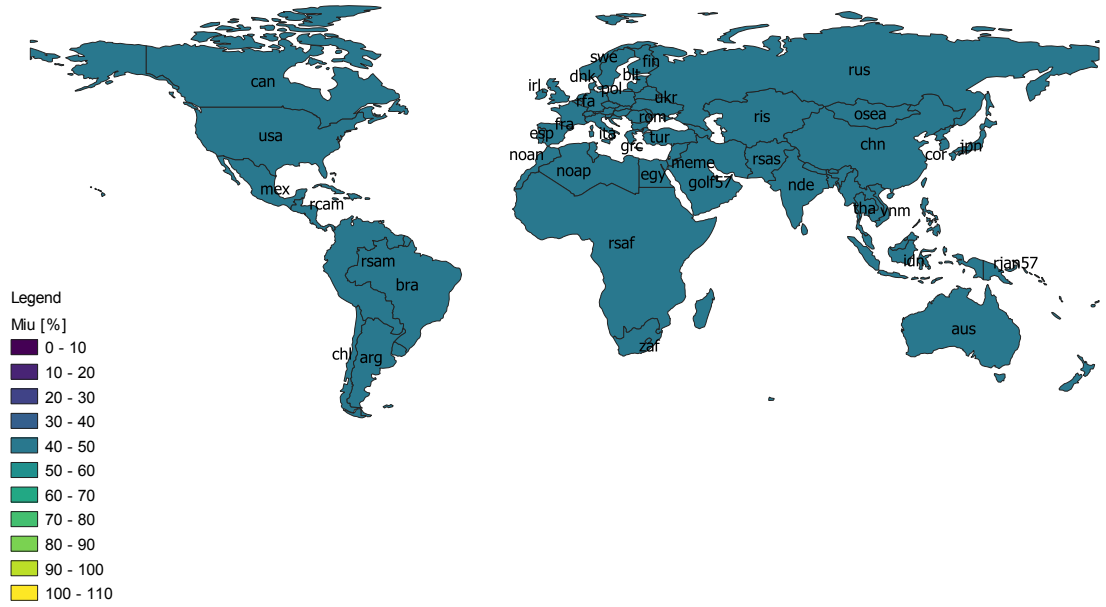

(a) *2030*

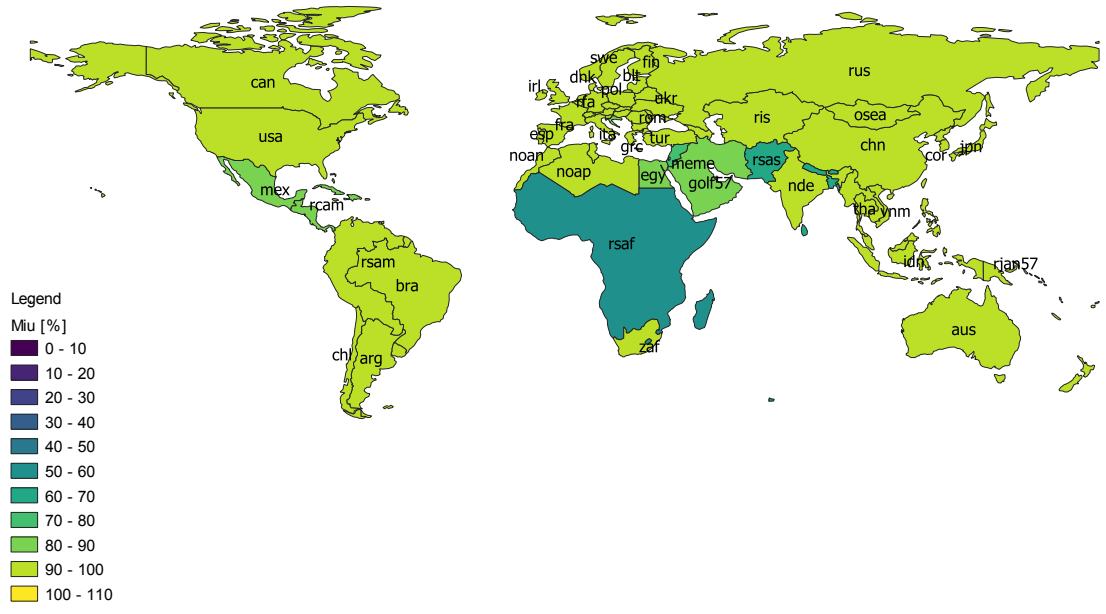

(b) *2050*

Figure 4.7: *Emission control rate maps of the Compromise solution for the years: (a) 2030, (b) 2050.*

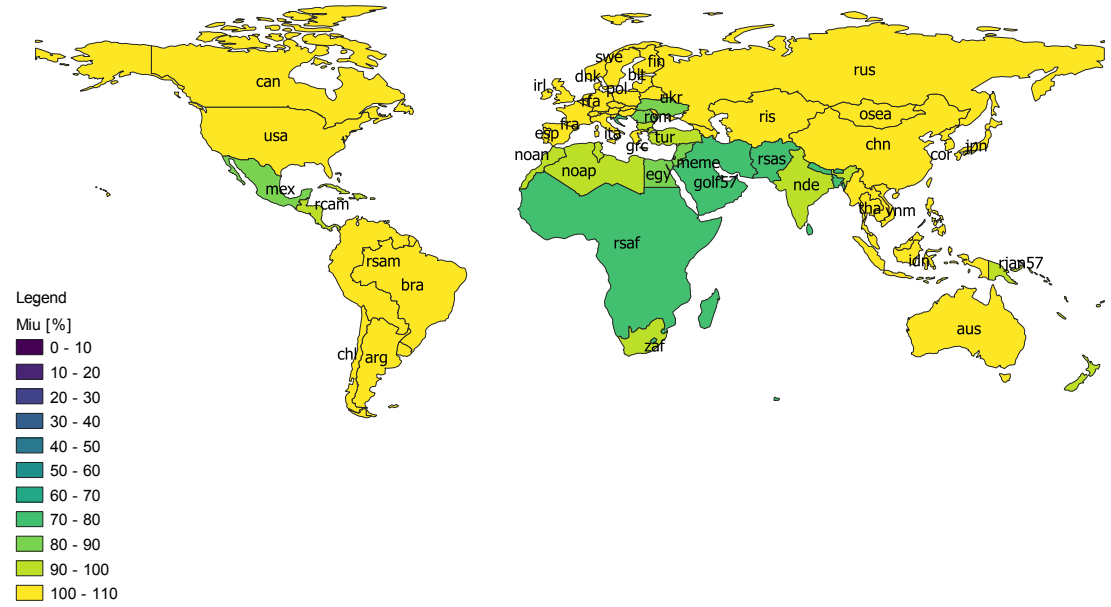

(a) *2080*

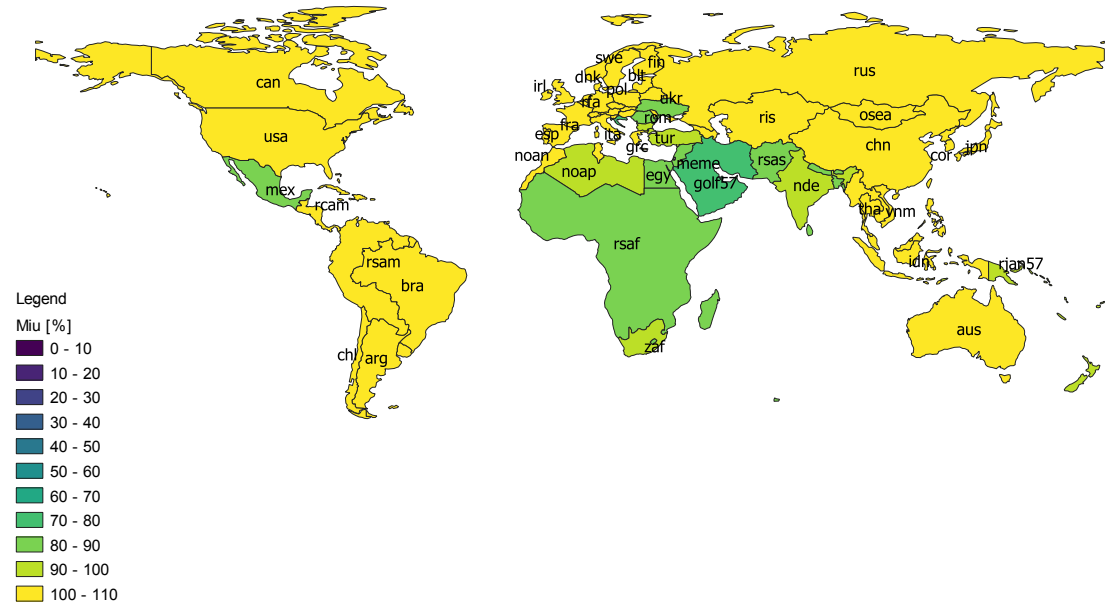

(b) *2100*

Figure 4.8: *Emission control rate maps of the Compromise solution for the years: (a) 2080, (b) 2100.*

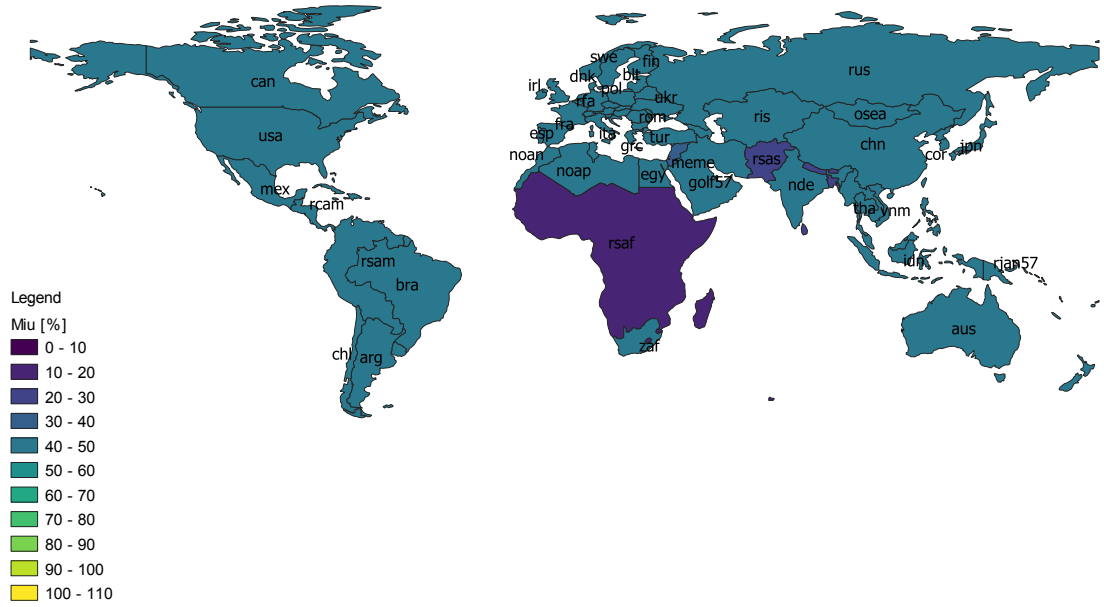

(a) *2030*

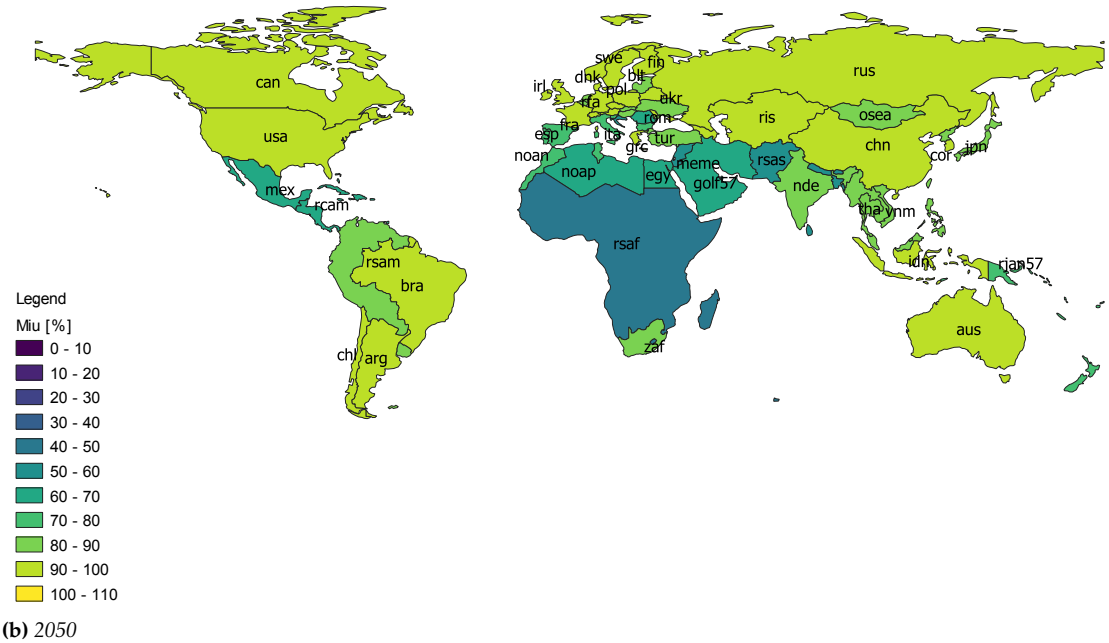

(b) *2050*

Figure 4.9: *Emission control rate maps of the Welfare solution for the years: (a) 2030, (b) 2050.*

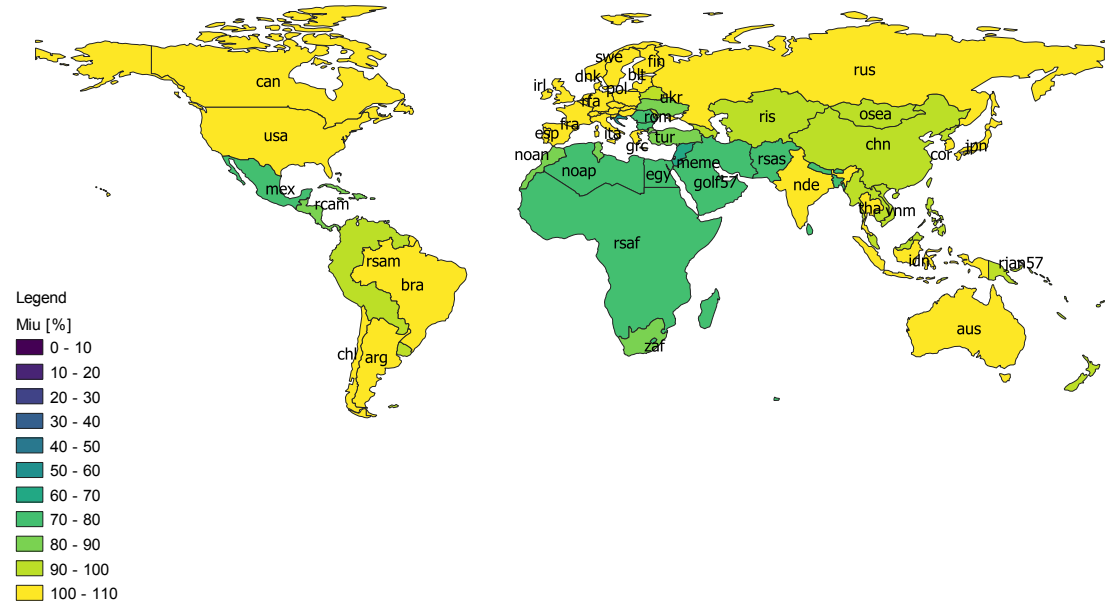

(a) *2080*

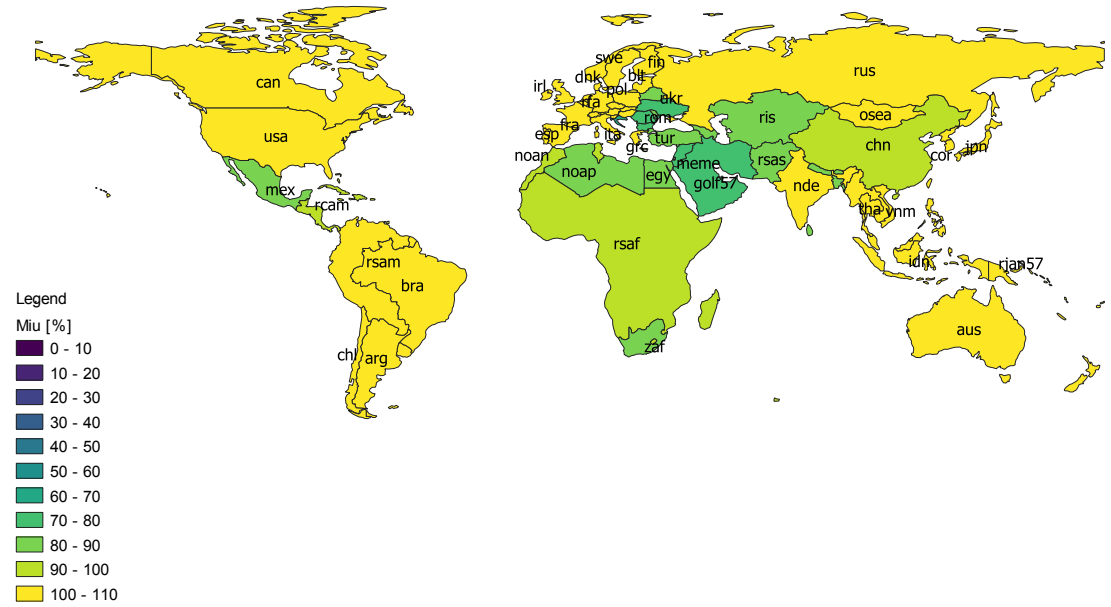

(b) *2100*

Figure 4.10: *Emission control rate maps of the Welfare solution for the years: (a) 2080, (b) 2100.*

The emission control rates of the Welfare solution are reported in Figure 4.9 and 4.10. In the year 2030, represented in Figure 4.9a, the majority of the regions have a 43% emission control rate. The few exceptions with a lower rate are regions like Sub-Saharan Africa and South Asia. From 2050 to 2080, the emission control rate increases in every region, similarly to the Compromise solution. In 2100, represented in Figure 4.10b, 39 out of 57 regions are already removing carbon out of the atmosphere. Like in the previous case, the regions around the tropical area have a lower emission control rate, between 60% and 97%.

We reported the emission control rates of the Temperature solution in Figure 4.11 and 4.12. Every region starts with miu of 43% in 2030, as shown in Figure 4.11a. In 2050, 47 regions out of 57 have an emission control rate of 100%. Of the 10 remaining regions, Sub-Saharan Africa has the lowest miu of 77%, while the values of the other regions lie between 87% and 99%. In 2080 every region reaches negative emissions. This does not change from 2080 to 2100, as Figure 4.12 shows. The Temperature solution represents the fastest and more decisive emission reduction policy. There is no differentiation between rich and poor regions: prioritizing the temperature objective requires strong emissions reductions for every region and this leaves no opportunity to consider inequality objectives.

In Figure 4.13 and 4.14 we represented the emission control rates of the 90/10 solution. Their emission reduction effort increase from 2030 to 2050 is lower than the other solutions. In 2050 only 34 regions have an emission control ratio of 100%. The emission control rate increase lightly in 2080 and 2100. As shown in Figure 4.14b, in 2100 only 35 regions reach negative emissions. The remaining regions have an emission reduction from 60% to 99%. In this solution, the differentiation between rich and poor regions is the most relevant. This result is coherent with a policy that results robust for the economic inequality objectives. Indeed, such policy requires the richest regions to reach negative emissions, while the worse-off ones bear a lower mitigation effort.

In conclusion, all selected robust solutions show a fast and immediate emission reductions. However, we highlighted a significant difference between the solutions, represented in terms of differentiation in the mitigation effort between regions. Since the regions in the tropical area tend to be poorer, a solution proposing an emission reduction policy robust with respect to inequality will project a mitigation effort significantly lower on those regions. This heterogeneity becomes smaller when taking into consideration solutions robust with respect to other objectives like the Compromise solution. Also, despite the high emission reductions required by every solution, scenarios leading to

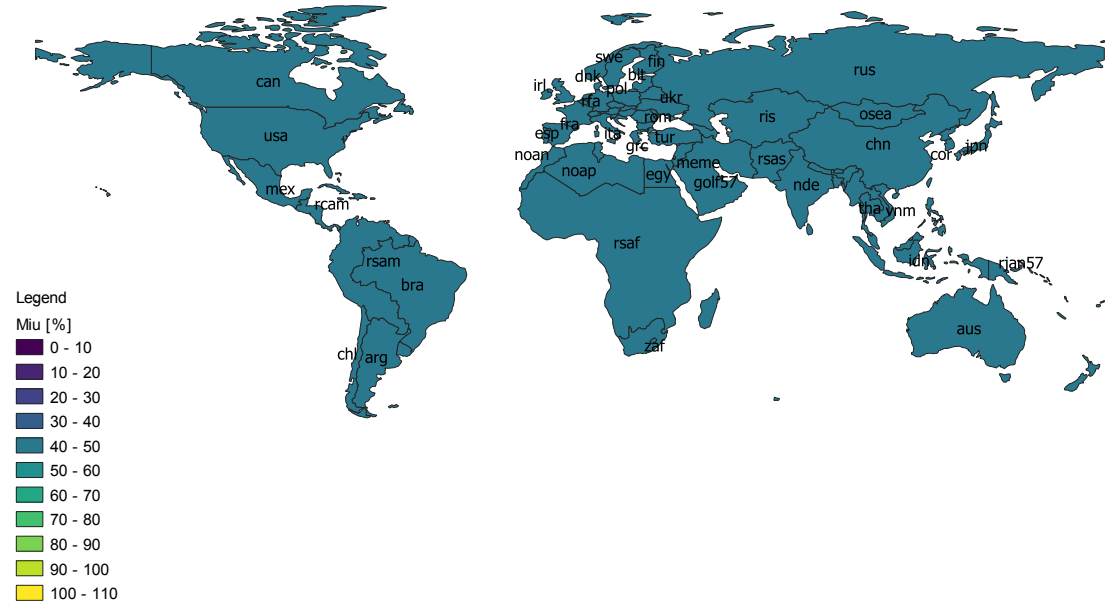

(a) *2030*

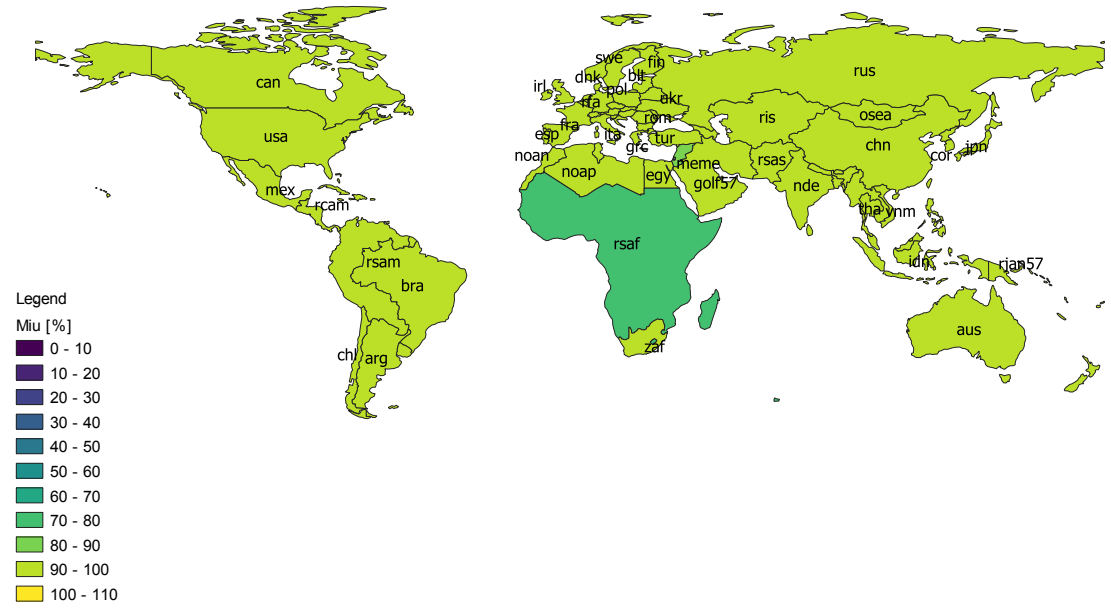

(b) *2050*

Figure 4.11: *Emission control rate maps of the Temperature solution for the years: (a) 2030, (b) 2050.*

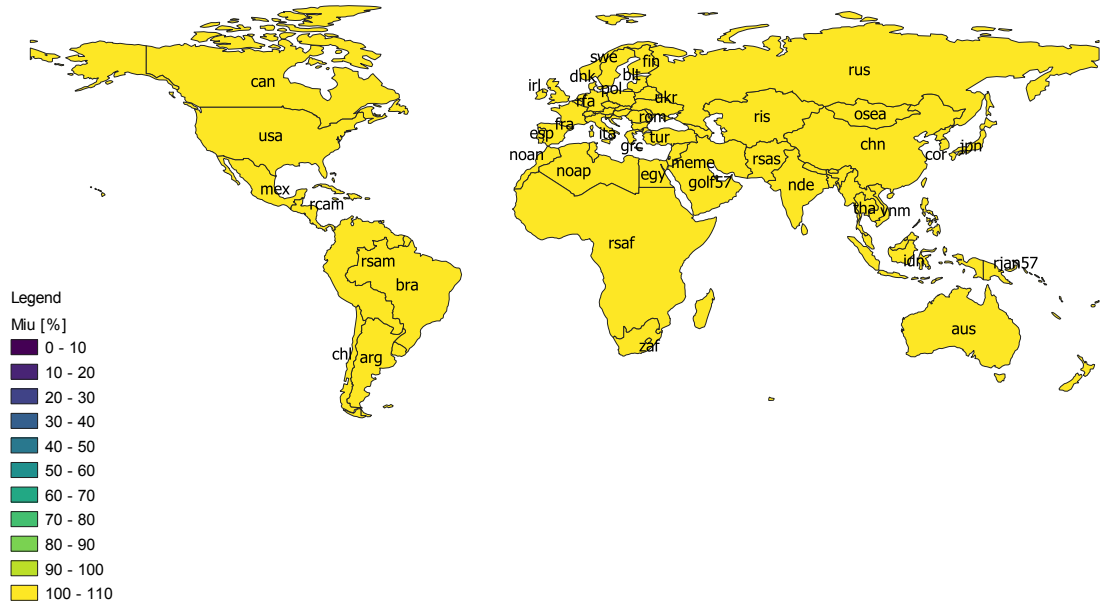

(a) *2080*

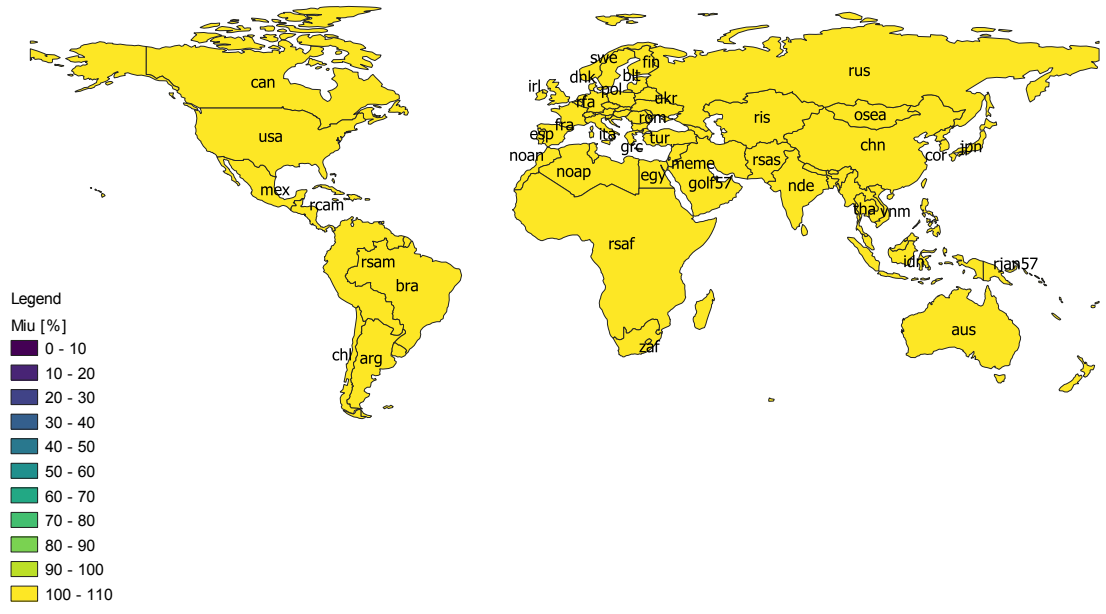

(b) *2100*

Figure 4.12: *Emission control rate maps of the Temperature solution for the years: (a) 2080, (b) 2100.*

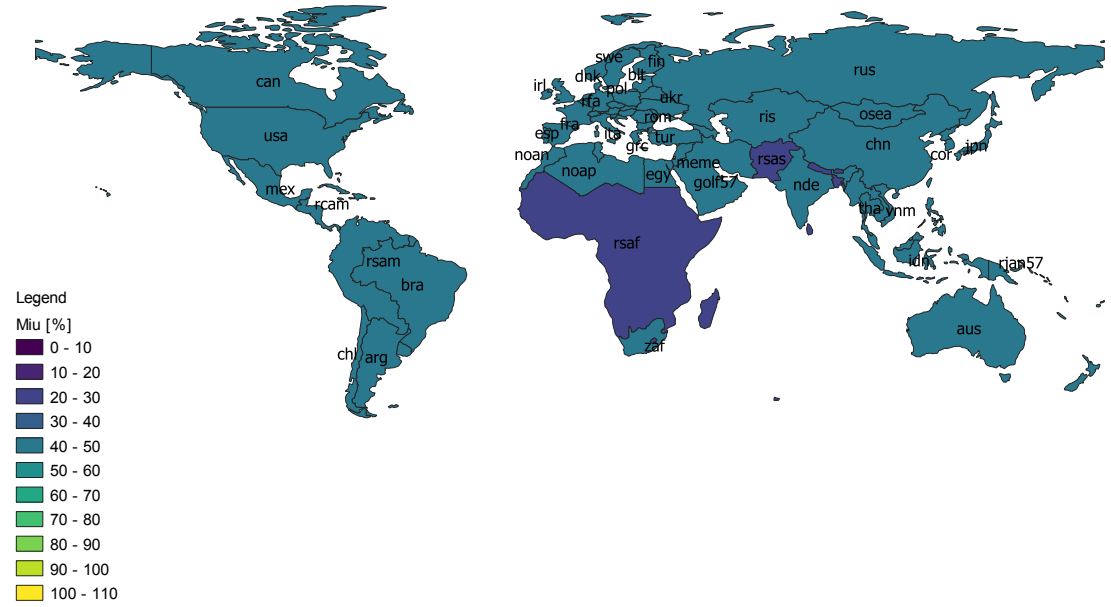

(a) *2030*

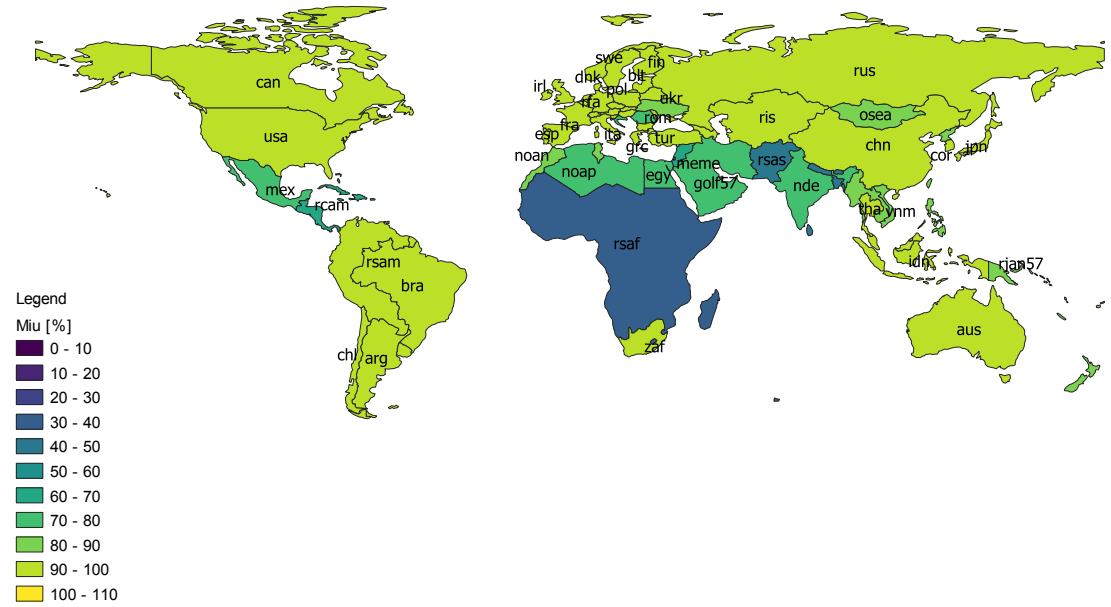

(b) *2050*

Figure 4.13: *Emission control rate maps of the 90/10 solution for the years: (a) 2030, (b) 2050.*

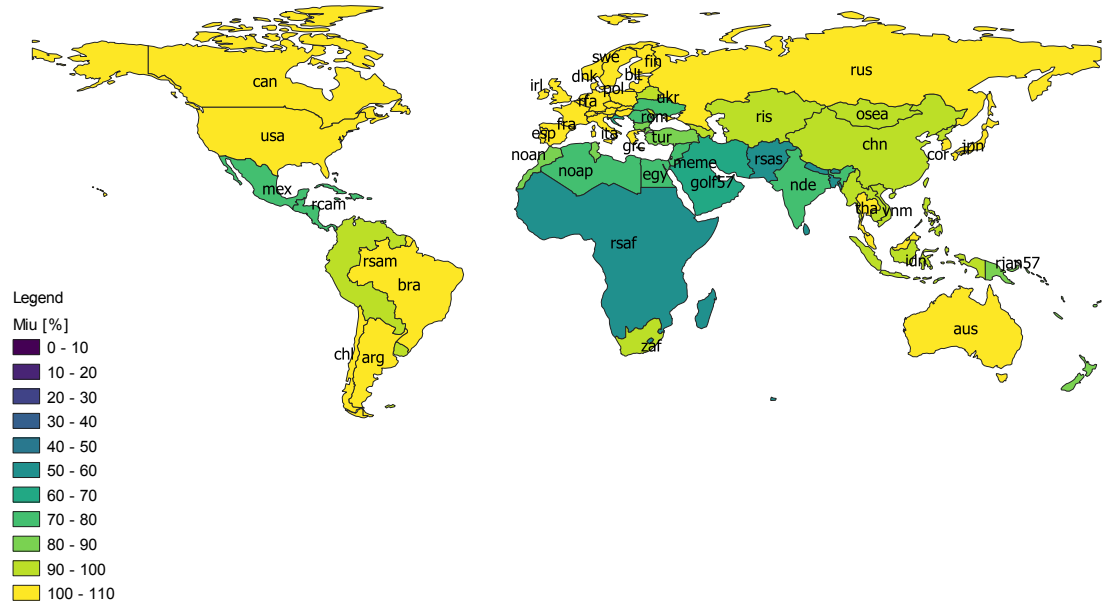

(a) *2080*

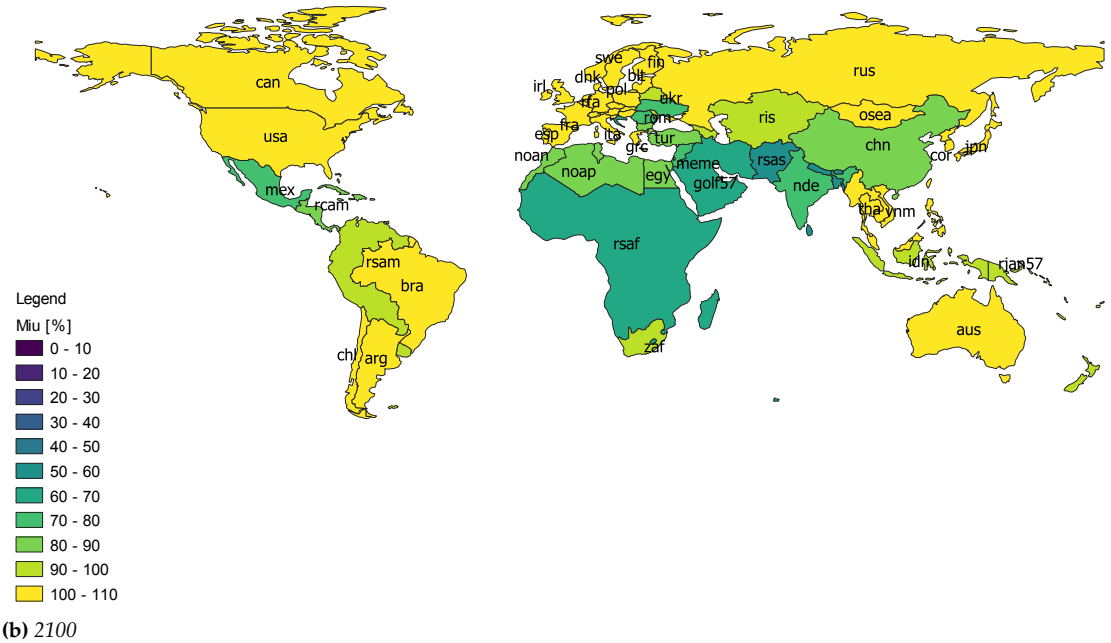

(b) *2100*

Figure 4.14: *Emission control rate maps of the 90/10 solution for the years: (a) 2080, (b) 2100.*

low welfare, high temperature and high inequality still remain.

5

Conclusions and future research

In this thesis, we explored relevant drivers of uncertainty of the RICE50+ CB-IAM and investigated the robustness of its assessed optimal Benefit-Cost climate policies. Our goals were:

1. To analyze how much do the narratives of the SSPs and the damage functions included in the RICE50+ model influence its optimal solutions;

2. To identify the high-risk scenarios with respect to the objectives considered and quantify the relevance of each driver of uncertainty in defining such scenarios;

3. To select a set of robust optimal solutions of the model over the considered scenarios, and analyze their emission abatement pathways.

We considered as objectives welfare, temperature increase and economic inequality, as explained in Section 3.3. First, we defined an ensemble of 60 scenarios resulting from the combination of the five SSPs, the six damage functions and the two Land-Use emissions cases. We re-simulated the emission control rates of 479 optimal solutions of the model and for each solution we obtained the objective values over the ensemble of scenarios. Then, we analyzed the performances of the solutions both over their original optimization scenario and the entire ensemble of scenarios to determine the influence of the SSPs narratives and damage functions' specification on the optimal solutions.

To identify the high-risk scenarios, we applied the PRIM algorithm. Its goal is to identify combinations of the input parameters that produce output values

larger (or smaller) than the global average. We applied the algorithm to two different cases:

1. the dataset obtained by the re-simulation of the RICE50+ solutions optimized with the CBA Land-Use emissions setting (see Section 3.2.5). For this case, we selected five input variables: the SSPs and impact functions used for the re-simulation, the rate of social time preference per year, the inequality aversion and the cooperation level.
2. The dataset obtained by the re-simulation of all the RICE50+ solutions optimized over the cooperative setting. For this case, we used all the input variables of the previous case, excluding the cooperation level.

As outputs, we utilized the most relevant objectives amongst the selected ones: welfare, the temperature in 2100 and the 90/10 income decile ratio. We then applied a resampling test to quantify the relevance of every input in defining the high-risk scenarios, as explained in Section 3.4.8.

To answer to our final research question, we performed a robustness analysis using the six robustness metrics explained in Section 3.5.1: maximin, maximax, mean-variance, PBS, PBP and LDC. After evaluating the robustness values, we implemented the two methods described in Section 3.6 to select a set of robust solutions. Lastly, we analyzed the optimal emission control rates of the selected robust solutions, representing the corresponding emission control rate maps in Section 4.3.2.

We first analyzed the influence of the SSPs narratives and damage functions specifications on the optimal RICE50+ solutions. As reported in Section 4.1.2, we showed that both the SSPs and the impact functions significantly affect the outcomes of the solutions. Furthermore, we highlighted the presence of scenarios that can lead to high welfare values and, simultaneously, to high economic inequality. Those scenarios may raise ethical and policy-relevant concerns about the distribution of climate impacts and mitigation efforts.

Through the application of PRIM we highlighted the presence of several high-risk scenarios associated to the SSPs and damage functions. In particular, in Section 4.2, we found scenarios of low welfare driven by SSP3, SSP4 and Kahn, BHM-LR and LRdiff damage functions. SSP2 and SSP5 resulted to be significant drivers for scenarios of high temperature. High inequality scenarios were always defined by SSP3 and SSP4, and by BHM-SR, SRdiff and DJO impact functions. We discussed the obtained results analyzing the narratives of the SSPs and the different formulations of the impact functions. In particular, the formulation of functions like DJO and BHM-SR leads to highly heterogeneous impacts which exacerbate inequalities.

Last, in Section 4.3, we identified four robust solutions: one for each of the relevant objectives and a solution of compromise across every objective. Furthermore, we analyzed the optimal emission reduction pathways of the selected solutions. The all depict a strong need for a fast and urgent reduction of the GHG emissions. However, these results suggest that this reduction should consider the existing economic inequalities as well as each country's responsibilities for historical GHG emissions.

To conclude, this work presents some limitations that could be addressed in future studies.

1. The analyses performed in this thesis could be applied considering a bigger ensemble of plausible future scenarios. Our application of PRIM evidenced the relevance of the parameters of inequality aversion and rate of social time preference per year in defining high-risk scenarios. Those parameters could be considered, together with the SSPs, the damage functions and the Land-Use emissions cases, to generate more possible future scenarios. Furthermore, different values of climate sensitivity could also be used to generate more scenarios.

2. The application of other methods could provide further insights on the results of this thesis. For example, the scenario discovery can be further explored by applying the CART method, mentioned in Section 3.4.3. The robustness analysis could also be repeated using different robustness metrics.

3. The analysis of robust climate policies could be expanded by applying the methods used in this thesis to the outputs of other IAMs.

4. This thesis provided robust emission reduction policies at a high level of geographical representation, based on the spatial scale of the RICE50+ model. However, because of the relevant economic inequalities, such reductions resulted in being strongly differentiated between regions. Because of this, further efforts should be spent to improve the spatial resolution of the IAMs used to optimize mitigation policies.

5. Lastly, future research should try to provide progress on the representation of economic inequality within countries, as well as other types of inequality, as reported in Section 2.5.

Bibliography

Aaheim, H. A., and C. B. Froyn (2001), Decision-making frameworks for climate policy under uncertainty, *CICERO Working Paper*.

Adler, M., D. Anthoff, V. Bosetti, G. Garner, K. Keller, and N. Treich (2017), Priority for the worse-off and the social cost of carbon, *Nature Climate Change*, *7*(6), 443–449, doi: 10.1038/nclimate3298.

Anthoff, D. (2009), Optimal global dynamic carbon taxation, *ESRI Working Paper 278*, Dublin.

Barnett, J. (2003), Security and climate change, *Global Environmental Change*, *13*(1), 7–17, doi: https://doi.org/10.1016/S0959-3780(02)00080-8.

Bosetti, V., E. Massetti, and M. Tavoni (2007), The WITCH model: structure, baseline, solutions, doi: https://dx.doi.org/10.2139/ssrn.960746.

Breiman, L., J. H. Friedman, R. A. Olshen, and C. J. Stone (2017), *Classification and regression trees*, Routledge, doi: https://doi.org/10.1201/9781315139470.

Bryant, B. P., and R. J. Lempert (2010), Thinking inside the box: A participatory, computer-assisted approach to scenario discovery, *Technological Forecasting and Social Change*, *77*(1), 34–49, doi: https://doi.org/10.1016/j.techfore.2009.08.002.

Burke, M., S. M. Hsiang, and E. Miguel (2015), Global non-linear effect of temperature on economic production, *Nature*, *527*(7577), 235–239, doi: 10.1038/nature15725.

Burke, M., W. M. Davis, and N. S. Diffenbaugh (2018), Large potential reduction in economic damages under UN mitigation targets, *Nature*, *557*(7706), 549–553, doi: https://doi.org/10.1038/s41586-018-0071-9.

Carleton, T. A., and S. M. Hsiang (2016), Social and economic impacts of climate, *Science*, *353*(6304), aad9837, doi: 10.1126/science.aad9837.

Chaturvedi, V., and P. R. Shukla (2014), Role of energy efficiency in climate change mitigation policy for India: assessment of co-benefits and opportunities within an integrated assessment modeling framework, *Climatic Change*, *123*(3), 597–609, doi: 10.1007/s10584-013-0898-x.

Dell, M., B. F. Jones, and B. A. Olken (2012), Temperature shocks and economic growth: Evidence from the last half century, *American Economic Journal: Macroeconomics*, *4*(3), 66–95, doi: 10.1257/mac.4.3.66.

Dennig, F., M. B. Budolfson, M. Fleurbaey, A. Siebert, and R. H. Socolow (2015), Inequality, climate impacts on the future poor, and carbon prices, *Proc Natl Acad Sci USA*, *112*(52), 15,827, doi: https://doi.org/10.1073/pnas.1513967112.

Diffenbaugh, N. S., and M. Burke (2019), Global warming has increased global economic inequality, *Proceedings of the National Academy of Sciences*, *116*(20), 9808–9813, doi: https://doi.org/10.1073/pnas.1816020116.

Drouet, L., V. Bosetti, and M. Tavoni (2015), Selection of climate policies under the uncertainties in the fifth assessment report of the IPCC, *Nature Climate Change*, *5*(10), 937–940, doi: 10.1038/nclimate2721.

Emmerling, J., and M. Tavoni (2021), Representing inequalities in integrated assessment modeling of climate change, *One Earth*, *4*(2), 177–180, doi: https://doi.org/10.1016/j.oneear.2021.01.013.

Feldstein, M. S. (1964), The social time preference discount rate in cost benefit analysis, *The Economic Journal*, *74*(294), 360–379, doi: https://doi.org/10.2307/2228484.

Fischer, C., and R. G. Newell (2008), Environmental and technology policies for climate mitigation, *Journal of Environmental Economics and Management*, *55*(2), 142–162, doi: https://doi.org/10.1016/j.jeem.2007.11.001.

Fisher-Vanden, K., and J. Weyant (2020), The Evolution of Integrated Assessment: Developing the Next Generation of Use-Inspired Integrated Assessment Tools, *Annual Review of Resource Economics*, *12*(1), 471–487, doi: 10.1146/annurev-resource-110119-030314.

Flues, F., and A. Thomas (2015), The distributional effects of energy taxes, (23), doi: https://doi.org/https://doi.org/10.1787/5js1qwkqqrbv-en.

Forster, P., T. Storelvmo, K. Armour, W. Collins, J. L. Dufresne, D. Frame, D. J. Lunt, T. Mauritsen, M. D. Palmer, M. Watanabe, M. Wild, and H. Zhang (2021), The Earth's Energy Budget, Climate Feedbacks, and Climate Sensitivity. In: Climate Change 2021: The Physical Science Basis. Contribution of Working Group I to the Sixth Assessment Report of the Intergovernmental Panel on Climate Change.

French, S. (1986), *Decision theory: an introduction to the mathematics of rationality*, Halsted Press.

Friedman, J. H., and N. I. Fisher (1999), Bump hunting in high-dimensional data, *Statistics and Computing*, *9*(2), 123–143, doi: 10.1023/A:1008894516817.

Garner, G., P. Reed, and K. Keller (2016), Climate risk management requires explicit representation of societal trade-offs, *Climatic Change*, *134*(4), 713–723, doi: 10.1007/s10584-016-1607-3.

Gastwirth, J. L. (1972), The Estimation of the Lorenz Curve and Gini Index, *The review of economics and statistics*, *54*(3), 306–316, doi: 10.2307/1937992.

Gazzotti, P., J. Emmerling, G. Marangoni, A. Castelletti, K.-I. van der Wijst, A. Hof, and M. Tavoni (2021), Persistent inequality in economically optimal climate policies, *Nature Communications*, *12*(1), 3421, doi: 10.1038/s41467-021-23613-y.

Gillingham, K., W. Nordhaus, D. Anthoff, G. Blanford, V. Bosetti, P. Christensen, H. McJeon, and J. Reilly (2018), Modeling Uncertainty in Integrated Assessment of Climate Change: A Multimodel Comparison, *Journal of the Association of Environmental and Resource Economists*, *5*(4), 791–826, doi: 10.1086/698910.

Giudici, F., A. Castelletti, M. Giuliani, and H. R. Maier (2020), An active learning approach for identifying the smallest subset of informative scenarios for robust planning under deep uncertainty, *Environmental Modelling & Software*, *127*, 104,681, doi: https://doi.org/10.1016/j.envsoft.2020.104681.

Giuliani, M., and A. Castelletti (2016), Is robustness really robust? how different definitions of robustness impact decision-making under climate change, *Climatic Change*, *135*(3-4), 409–424, doi: https://doi.org/10.1007/s10584-015-1586-9.

Glanemann, N., S. N. Willner, and A. Levermann (2020), Paris climate agreement passes the cost-benefit test, *Nature Communications*, *11*(1), 110, doi: 10.1038/s41467-019-13961-1.

Hall, J. W., R. J. Lempert, K. Keller, A. Hackbarth, C. Mijere, and D. J. McInerney (2012), Robust climate policies under uncertainty: A comparison of robust decision making and info-gap methods, *Risk Analysis*, *32*(10), 1657–1672, doi: https://doi.org/10.1111/j.1539-6924.2012.01802.x.

Hallegatte, S., and J. Rozenberg (2017), Climate change through a poverty lens, *Nature Climate Change*, *7*(4), 250–256, doi: 10.1038/nclimate3253.

Hänsel, M. C., M. A. Drupp, D. J. A. Johansson, F. Nesje, C. Azar, M. C. Freeman, B. Groom, and T. Sterner (2020), Climate economics support for the un climate targets, *Nature Climate Change*, *10*(8), 781–789, doi: 10.1038/s41558-020-0833-x.

Hope, C. (2011), The social cost of CO2 from the PAGE09 model, *Economics discussion paper*, (2011-39), doi: https://dx.doi.org/10.2139/ssrn.1973863.

Howard, P. H., and T. Sterner (2017), Few and not so far between: A meta-analysis of climate damage estimates, *Environmental and Resource Economics*, *68*(1), 197–225, doi: 10.1007/s10640-017-0166-z.

Howell, S. T. (2017), Financing innovation: Evidence from R&D grants, *American Economic Review*, *107*(4), 1136–64, doi: 10.1257/aer.20150808.

IPCC (2013), *Climate Change 2013: The Physical Science Basis. Contribution of Working Group I to the Fifth Assessment Report of the Intergovernmental Panel on Climate Change*, 1535 pp., Cambridge University Press, Cambridge, United Kingdom and New York, NY, USA, doi: 10.1017/CBO9781107415324.

IPCC (2021a), Climate Change 2021: The Physical Science Basis. Contribution of Working Group I to the Sixth Assessment Report of the Intergovernmental Panel on Climate Change.

IPCC (2021b), Summary for Policymakers. In: Climate Change 2021: The Physical Science Basis. Contribution of Working Group I to the Sixth Assessment Report of the Intergovernmental Panel on Climate Change.

Jekabsons, G. (2015), Bump Hunting using Patient Rule Induction Method for Matlab/Octave, `http://www.cs.rtu.lv/jekabsons/`, [Online; accessed 18/08/2021].

Jonathan, D. H., M. R. Patrick, B. Z. Harrison, and W. C. Gregory (2015), How should robustness be defined for water systems planning under change?, *Journal of Water Resources Planning and Management*, *141*(10), 04015,012, doi: 10.1061/(ASCE)WR.1943-5452.0000509.

Kahn, M. E., K. Mohaddes, R. N. Ng, M. H. Pesaran, M. Raissi, and J.-C. Yang (2019), Long-term macroeconomic effects of climate change: A cross-country analysis, *National Bureau of Economic Research*, doi: 10.3386/w26167.

Kasprzyk, J. R., S. Nataraj, P. M. Reed, and R. J. Lempert (2013), Many objective robust decision making for complex environmental systems undergoing change, *Environmental Modelling & Software*, *42*, 55–71, doi: https://doi.org/10.1016/j.envsoft.2012.12.007.

Kemfert, C. (2005), Induced technological change in a multi-regional, multi-sectoral, integrated assessment model (WIAGEM): Impact assessment of climate policy strategies, *Ecological Economics*, *54*(2), 293–305, doi: https://doi.org/10.1016/j.ecolecon.2004.12.031, Technological Change and the Environment.

King, A. D., and L. J. Harrington (2018), The inequality of climate change from 1.5 to 2 C of global warming, *Geophysical Research Letters*, *45*(10), 5030–5033, doi: https://doi.org/10.1029/2018GL078430.

Knight, F. H. (1921), *Risk, uncertainty and profit*, vol. 31, Houghton Mifflin.

Kwakkel, J. H. (2019), A generalized many-objective optimization approach for scenario discovery, *FUTURES & FORESIGHT SCIENCE*, *1*(2), e8, doi: https://doi.org/10.1002/ffo2.8.

Kwakkel, J. H., and M. Jaxa-Rozen (2016), Improving scenario discovery for handling heterogeneous uncertainties and multinomial classified outcomes, *Environmental Modelling & Software*, *79*, 311–321, doi: https://doi.org/10.1016/j.envsoft.2015.11.020.

Kwakkel, J. H., S. Eker, and E. Pruyt (2016), *How Robust is a Robust Policy? Comparing Alternative Robustness Metrics for Robust Decision-Making*, pp. 221–237, Robustness Analysis in Decision Aiding, Optimization, and Analytics, Springer International Publishing, Cham, doi: 10.1007/978-3-319-33121-8_10.

Lempert, R. J., D. G. Groves, S. W. Popper, and S. C. Bankes (2006), A general, analytic method for generating robust strategies and narrative scenarios, *Management science*, *52*(4), 514–528, doi: 10.1287/mnsc.1050.0472.

Lempert, R. J., B. P. Bryant, and S. C. Bankes (2008), *Comparing Algorithms for Scenario Discovery*, RAND Corporation.

Maier, H. R., J. H. A. Guillaume, H. van Delden, G. A. Riddell, M. Haasnoot, and J. H. Kwakkel (2016), An uncertain future, deep uncertainty, scenarios, robustness and adaptation: How do they fit together?, *Environmental Modelling & Software*, *81*, 154–164, doi: https://doi.org/10.1016/j.envsoft.2016.03.014.

Marangoni, G., J. R. Lamontagne, J. D. Quinn, P. M. Reed, and K. Keller (2021), Adaptive mitigation strategies hedge against extreme climate futures, *Climatic Change*, *166*(3), 37, doi: 10.1007/s10584-021-03132-x.

McInerney, D., R. Lempert, and K. Keller (2012), What are robust strategies in the face of uncertain climate threshold responses?, *Climatic Change*, *112*(3), 547–568, doi: https://doi.org/10.1007/s10584-011-0377-1.

McPhail, C., H. R. Maier, J. H. Kwakkel, M. Giuliani, A. Castelletti, and S. Westra (2018), Robustness metrics: How are they calculated, when should they be used and why do they give different results?, *Earth's Future*, *6*(2), 169–191, doi: https://doi.org/10.1002/2017EF000649.

McPhail, C., H. R. Maier, S. Westra, J. H. Kwakkel, and L. van der Linden (2020), Impact of scenario selection on robustness, *Water Resources Research*, *56*(9), e2019WR026,515, doi: https://doi.org/10.1029/2019WR026515.

Mendelsohn, R., A. Dinar, and L. Williams (2006), The distributional impact of climate change on rich and poor countries, *Environment and development economics*, *11*(2), 159–178, doi: 10.1017/S1355770X05002755.

Milanovic, B. (2011), *Worlds Apart: Measuring International and Global Inequality*, Princeton University Press, doi: 10.1515/9781400840816.

Moore, F. C., and D. B. Diaz (2015), Temperature impacts on economic growth warrant stringent mitigation policy, *Nature Climate Change*, *5*(2), 127–131, doi: https://doi.org/10.1038/nclimate2481.

Moore, F. C., U. Baldos, T. Hertel, and D. Diaz (2017), New science of climate change impacts on agriculture implies higher social cost of carbon, *Nature communications*, *8*(1), 1–9, doi: https://doi.org/10.1038/s41467-017-01792-x.

Nannings, B., A. Abu-Hanna, and E. de Jonge (2008), Applying PRIM (Patient Rule Induction Method) and logistic regression for selecting high-risk subgroups in very elderly ICU patients, *International Journal of Medical Informatics*, *77*(4), 272–279, doi: https://doi.org/10.1016/j.ijmedinf.2007.06.007.

Nielsen, K. S., K. A. Nicholas, F. Creutzig, T. Dietz, and P. C. Stern (2021), The role of high-socioeconomic-status people in locking in or rapidly reducing energy-driven greenhouse gas emissions, *Nature Energy*, doi: 10.1038/s41560-021-00900-y.

Nordhaus, W. (2007a), Critical Assumptions in the Stern Review on Climate Change, *Science*, *317*(5835), 201–202, doi: 10.1126/science.1137316.

Nordhaus, W. (2018), Projections and uncertainties about climate change in an era of minimal climate policies, *American Economic Journal: Economic Policy*, *10*(3), 333–60, doi: 10.1257/pol.20170046.

Nordhaus, W. D. (1993), Rolling the 'DICE': an optimal transition path for controlling greenhouse gases, *Resource and Energy Economics*, *15*(1), 27–50, doi: https://doi.org/10.1016/0928-7655(93)90017-O.

Nordhaus, W. D. (1994), Expert opinion on climatic change, *American Scientist*, *82*(1), 45–51.

Nordhaus, W. D. (2007b), A Review of the Stern Review on the Economics of Climate Change, *Journal of Economic Literature*, *45*(3), 686–702, doi: 10.1257/jel.45.3.686.

Nordhaus, W. D., and Z. Yang (1996), A regional dynamic general-equilibrium model of alternative climate-change strategies, *The American Economic Review*, *86*(4), 741–765.

O'Neill, B. C., E. Kriegler, K. L. Ebi, E. Kemp-Benedict, K. Riahi, D. S. Rothman, B. J. van Ruijven, D. P. van Vuuren, J. Birkmann, K. Kok, M. Levy, and W. Solecki (2017), The roads ahead: Narratives for shared socioeconomic pathways describing world futures in the 21st century, *Global Environmental Change*, *42*, 169–180, doi: https://doi.org/10.1016/j.gloenvcha.2015.01.004.

Peñasco, C., L. D. Anadón, and E. Verdolini (2021), Systematic review of the outcomes and trade-offs of ten types of decarbonization policy instruments, *Nature Climate Change*, *11*(3), 257–265, doi: https://doi.org/10.1038/s41558-020-00971-x.

Peterson, E. W. (2017), Is economic inequality really a problem? A review of the arguments, doi: 10.3390/socsci6040147.

Pflug, G. C. (2000), *Some Remarks on the Value-at-Risk and the Conditional Value-at-Risk*, pp. 272–281, Springer US, Boston, MA, doi: 10.1007/978-1-4757-3150-7_15.

Pindyck, R. S. (2013), Climate change policy: What do the models tell us?, *Journal of Economic Literature*, *51*(3), 860–72, doi: 10.1257/jel.51.3.860.

Pindyck, R. S. (2017), The use and misuse of models for climate policy, *Review of Environmental Economics and Policy*, *11*(1), 100–114, doi: 10.1093/reep/rew012.

Pindyck, R. S. (2019), The social cost of carbon revisited, *Journal of Environmental Economics and Management*, *94*, 140–160, doi: https://doi.org/10.1016/j.jeem.2019.02.003.

Porter, M. D., and D. E. Brown (2007), Detecting local regions of change in high-dimensional criminal or terrorist point processes, *Computational statistics & data analysis*, *51*(5), 2753–2768, doi: https://doi.org/10.1016/j.csda.2006.07.002.

Rao, N. D., B. J. van Ruijven, K. Riahi, and V. Bosetti (2017), Improving poverty and inequality modelling in climate research, *Nature Climate Change*, *7*(12), 857–862, doi: 10.1038/s41558-017-0004-x.

Reilly, J., S. Paltsev, K. Strzepek, N. E. Selin, Y. Cai, K.-M. Nam, E. Monier, S. Dutkiewicz, J. Scott, M. Webster, and A. Sokolov (2013), Valuing climate impacts in integrated assessment models: the MIT IGSM, *Climatic Change*, *117*(3), 561–573, doi: 10.1007/s10584-012-0635-x.

Riahi, K., D. P. van Vuuren, E. Kriegler, J. Edmonds, B. C. O,ÄôNeill, S. Fujimori, N. Bauer, K. Calvin, R. Dellink, O. Fricko, W. Lutz, A. Popp, J. C. Cuaresma, S. KC, M. Leimbach, L. Jiang, T. Kram, S. Rao, J. Emmerling, K. Ebi, T. Hasegawa, P. Havlik, F. Humpenüder, L. A. D. Silva, S. Smith, E. Stehfest, V. Bosetti, J. Eom, D. Gernaat, T. Masui, J. Rogelj, J. Strefler, L. Drouet, V. Krey, G. Luderer, M. Harmsen, K. Takahashi, L. Baumstark, J. C. Doelman, M. Kainuma, Z. Klimont, G. Marangoni, H. Lotze-Campen, M. Obersteiner, A. Tabeau, and M. Tavoni (2017), The Shared Socioeconomic Pathways and their energy, land use, and greenhouse gas emissions implications: An overview, *Global Environmental Change*, *42*, 153–168, doi: https://doi.org/10.1016/j.gloenvcha.2016.05.009.

Rozenberg, J., C. Guivarch, R. Lempert, and S. Hallegatte (2014), Building SSPs for climate policy analysis: a scenario elicitation methodology to map the space of possible future challenges to mitigation and adaptation, *Climatic Change*, *122*(3), 509–522, doi: 10.1007/s10584-013-0904-3.

Sala-i Martin, X. (2006), The world distribution of income: Falling poverty and... convergence, period, *The Quarterly Journal of Economics*, *121*(2), 351–397, doi: 10.1162/qjec.2006.121.2.351.

Savage, L. J. (1951), The theory of statistical decision, *null*, *46*(253), 55–67, doi: 10.1080/01621459.1951.10500768.

Scrimgeour, F., L. Oxley, and K. Fatai (2005), Reducing carbon emissions? The relative effectiveness of different types of environmental tax: The case of New Zealand, *Environmental Modelling & Software*, *20*(11), 1439–1448, doi: https://doi.org/10.1016/j.envsoft.2004.09.024.

Simon, H. A. (1956), Rational choice and the structure of the environment., *Psychological review*, *63*(2), 129, doi: https://psycnet.apa.org/doi/10.1037/h0042769.

Sofuoğlu, E., and A. Ay (2020), The relationship between climate change and political instability: the case of MENA countries (1985: 01–2016: 12), *Environmental Science and Pollution Research*, pp. 1–11, doi: https://doi.org/10.1007/s11356-020-07937-8.

Song, H., D. B. Kemp, L. Tian, D. Chu, H. Song, and X. Dai (2021), Thresholds of temperature change for mass extinctions, *Nature Communications*, *12*(1), 4694, doi: 10.1038/s41467-021-25019-2.

Stehfest, E., D. van Vuuren, L. Bouwman, and T. Kram (2014), *Integrated assessment of global environmental change with IMAGE 3.0: Model description and policy applications*, Netherlands Environmental Assessment Agency (PBL).

Stern, N. (2006), *Stern Review: The economics of climate change*.

Stern, N. (2014a), Ethics, equity and the economics of climate change paper 1: Science and philosophy, *Economics and Philosophy*, *30*(3), 397–444, doi: 10.1017/S0266267114000297.

Stern, N. (2014b), Ethics, equity and the economics of climate change paper 2: Economics and politics, *Economics and Philosophy*, *30*(3), 445–501, doi: 10.1017/S0266267114000303.

Stern, N., and C. Taylor (2007), Climate Change: Risk, Ethics, and the Stern Review, *Science*, *317*(5835), 203–204, doi: 10.1126/science.1142920.

Taconet, N., A. Méjean, and C. Guivarch (2020), Influence of climate change impacts and mitigation costs on inequality between countries, *Climatic Change*, *160*(1), 15–34, doi: https://doi.org/10.1007/s10584-019-02637-w.

Ueckerdt, F., R. Pietzcker, Y. Scholz, D. Stetter, A. Giannousakis, and G. Luderer (2017), Decarbonizing global power supply under region-specific consideration of challenges and options of integrating variable renewables in the REMIND model, *Energy Economics*, *64*, 665–684, doi: https://doi.org/10.1016/j.eneco.2016.05.012.

Ueckerdt, F., K. Frieler, S. Lange, L. Wenz, G. Luderer, and A. Levermann (2019), The economically optimal warming limit of the planet, *Earth System Dynamics*, *10*(4), 741–763, doi: 10.5194/esd-10-741-2019.

UNFCCC (2015), Adoption of the Paris Agreement. I: Proposal by the president. draft decision cp.21, *Tech. rep*.

van der Wijst, K.-I., A. F. Hof, and D. P. van Vuuren (2021), On the optimality of 2° C targets and a decomposition of uncertainty, *Nature communications*, *12*(1), 1–11, doi: https://doi.org/10.1038/s41467-021-22826-5.

Voudouris, V., K. Matsumoto, J. Sedgwick, R. Rigby, D. Stasinopoulos, and M. Jefferson (2014), Exploring the production of natural gas through the lenses of the ACEGES model, *Energy Policy*, *64*, 124–133, doi: https://doi.org/10.1016/j.enpol.2013.08.053.

Wald, A. (1949), Statistical decision functions, *The Annals of Mathematical Statistics*, *20*(2), 165–205, doi: 10.1214/aoms/1177730030.

Weitzman, M. L. (2012), GHG Targets as Insurance Against Catastrophic Climate Damages, *Journal of Public Economic Theory*, *14*(2), 221–244, doi: https://doi.org/10.1111/j.1467-9779.2011.01539.x.

Weyant, J. (2014), Integrated assessment of climate change: state of the literature, *Journal of Benefit-Cost Analysis*, *5*(3), 377–409, doi: 10.1515/jbca-2014-9002.

Weyant, J. (2017), Some Contributions of Integrated Assessment Models of Global Climate Change, *Review of Environmental Economics and Policy*, *11*(1), 115–137, doi: 10.1093/reep/rew018.

Weyant, J., O. Davidson, H. Dowlatabadi, J. Edmonds, M. Grubb, E. Parson, R. Richels, J. Rotmans, P. Shukla, R. S. Tol, et al. (1995), Integrated assessment of climate change: an overview and comparison of approaches and results, *Climate change*, *3*.

A

Additional material

A.1 Scenario discovery analysis of all the set of solutions

In this section, we report the results of the application of PRIM on the CBA-subset and the related considerations. In Figure A.1 we represented the results on the validation set for welfare, temperature in 2100 and 90/10 ratio.

By applying PRIM to the welfare objective represented in Figure A.1a, we found four boxes with average welfare from 0.57 to 0.69, lower than the global average of 0.77. The boxes cover from 10% to 11% of the dataset. According to the resampling test, the significant inputs are the SSPs, the damage functions, the inequality aversion and the cooperation level. Amongst the SSPs, SSP3 and SSP4 are the most relevant in defining high-risk scenarios because of their narratives of low economic growth. The algorithm selected all the damage functions, but the most relevant are BHM-LRdiff, Kahn and the DJO functions. The first two are damage functions that project impacts on rich and poor countries alike, therefore leading to low welfare values. The DJO function has a negative effect only on poor countries, as explained in Section 3.2.3. These impacts affect only part of the world's regions; however, they are sufficient to lead to scenarios of below-average welfare, especially when coupled with the slow economic development of SSP3. The algorithm also selected as rule all inequality aversion levels from the absence of inequality aversion (non-cooperative solutions) to the value 1.45. The remaining value of 2 represents a very high inequality aversion, as reported in Table 3.1. This rule shows that a low level of inequality aversion can undermine the possibility of achieving high welfare scenarios.

The non-cooperative setting is also a relevant driver leading to high-risk scenarios. This rule highlight the importance of international cooperation in avoiding scenarios that result in unsatisfactory welfare values.

Our analysis of temperature in 2100, reported in Figure A.1b, resulted in four boxes with an average temperature higher than the global average. The boxes cover from 10% to 11% of the dataset. All the inputs are significant, based on the results of the resampling test. The SSP2, SSP3 and SSP5 are the most significant drivers to high temperature scenarios. The narrative of the SSP5 is of strong development based on the exploitation of fossil fuels and lack of environmental concern, so it can pose high challenges to mitigation efforts and result in scenarios of high temperature. The SSP3 also project a relevant use of fossil fuels, together with disregard for the environmental concerns. This results in environmental degradation and scenarios with high temperatures. The SSP2 narrative is better than the first two concerning the environmental issue, but it still projects the use of fossil fuels. This can explain why it has been selected as a significant input for high temperature scenarios. The algorithm selected all the damage functions except Kahn and all the levels of the rate of social time preference. The most relevant value is the highest: 0.03. This value represents a society that gives importance to the consumptions in present times, and less relevance to the consumptions in future points in time. The preference is translated into fewer concerns for the future generations, therefore it leads more easily to high-risk scenarios. Just as in the previous case, the algorithm selected the low levels of inequality aversion and the non-cooperative setting as relevant inputs leading to high unsatisfactory scenarios. These rules again show the relevance of the economic inequality issue and the international cooperation in leading to high-risk scenarios.

By applying PRIM to the 90/10 ratio objective represented in Figure A.1c, we obtained two boxes with an average ratio of 15.90 and 30.31, higher than the global average of 9.16. The boxes cover 12% and 11% of the dataset respectively. The significant drivers are the SSPs, the damage functions and the cooperation level. Concerning the SSP, SSP3-5 have been selected, with SSP4 being the most relevant. We expected a similar result result since the SSP4 describes specifically a pathway of increasing inequalities between countries. As relevant damage functions, the algorithm selected all the functions but Kahn and BHM-LR. Those two functions are the ones projecting negative impacts more evenly, while the selected ones tend to project an uneven distribution of damages, as previously discussed. This is, understandably, a driver for scenarios of high inequality. The last significant input is again the cooperation level: a non-cooperative setting leads to high-risk scenarios with respect to inequality.

	SSP					Damage function						Prstp			Inequality aversion					Cooperation level		Mean	Support
	SSP1	SSP2	SSP3	SSP4	SSP5	BHM-SR	BHM-LR	BHM-SRdiff	BHM-LRdiff	DJO	Kahn	0.001	0.015	0.03	\	0	0.5	1.45	2	Coop	Non-coop	0.77	13470
Box 1		■	■	■			■	■	■	■	■										■	0.57	0.10
Box 2			■				■		■	■	■											0.50	0.11
Box 3			■	■		■			■	■	■				■	■	■	■				0.66	0.11
Box 4			■	■																		0.69	0.11
Leftovers																						0.89	0.57
Significance	100%					100%						23.3%			50%					93.3%			

(a) *Welfare*

	SSP					Damage function						Prstp			Inequality aversion					Cooperation level		Mean	Support
	SSP1	SSP2	SSP3	SSP4	SSP5	BHM-SR	BHM-LR	BHM-SRdiff	BHM-LRdiff	DJO	Kahn	0.001	0.015	0.03	\	0	0.5	1.45	2	Coop	Non-coop	2.09	13470
Box 1		■	■	■	■								■	■							■	3.21	0.11
Box 2		■	■		■	■	■	■	■	■		■		■	■	■						2.50	0.10
Box 3														■	■	■	■					2.20	0.11
Box 4	■	■	■		■										■	■						2.17	0.11
Leftovers																						1.76	0.57
Significance	96.7%					70%						100%			100%					100%			

(b) *Temperature in 2100*

	SSP					Damage function						Prstp			Inequality aversion					Cooperation level		Mean	Support
	SSP1	SSP2	SSP3	SSP4	SSP5	BHM-SR	BHM-LR	BHM-SRdiff	BHM-LRdiff	DJO	Kahn	0.001	0.015	0.03	\	0	0.5	1.45	2	Coop	Non-coop	9.16	13470
Box 1			■	■	■																■	15.90	0.12
Box 2				■		■		■	■	■												30.31	0.11
Leftovers																						5.08	0.77
Significance	100%					100%						10%			33.3%					96.7%			

(c) *90/10 ratio*

Figure A.1: *Results of the PRIM analysis on: (a) welfare, (b) temperature in 2100, (c) 90/10 ratio. On the columns there are the inputs, on the rows the boxes. The red cells represent the rules of the boxes. In the last two columns there are mean and support of each box. The results of the resampling test are in the last row expressed as significance.*

A.2 Emission control rates

Here we report the set of emission control rates of the four robust solutions we selected in Section 4.3. The data are referred to every region of the RICE50+ model for the years 2030, 2050, 2080 and 2100. Table A.1 refers to the Compromise solution, table A.2 to the Welfare solution, table A.3 to the Temperature solution and table A.4 to the 90/10 solution.

Table A.1: *Emission control rates of the Compromise solution, referred to every region in the years 2030, 2050, 2080 and 2100.*

Region	2030 [%]	2050 [%]	2080 [%]	2100 [%]
arg	43	100	103.45	106.21
aus	43	100	103.45	106.21
aut	43	100	103.45	106.21
bel	43	100	103.45	106.21
bgr	43	100	94.63	94.64
blt	43	100	103.45	106.21
bra	43	100	103.45	106.21
can	43	100	103.45	106.21
chl	43	100	103.45	106.21
chn	43	100	103.45	102.39
cor	43	100	103.45	106.21
cro	43	83.46	77.03	77.77
dnk	43	100	103.45	106.21
egy	43	81.79	84.51	88.76
esp	43	100	103.45	106.21
fin	43	100	103.45	106.21
fra	43	100	103.45	106.21
gbr	43	100	103.45	106.21
golf57	43	85.61	76.53	75.1
grc	43	100	103.45	106.21
hun	43	100	103.45	106.21
idn	43	100	103.45	106.21
irl	43	100	103.45	106.21
ita	43	100	103.45	106.21
jpn	43	100	103.45	106.21
meme	43	79.41	81.2	85.53

Continued on next page

Table A.1: *Emission control rates of the Compromise solution, referred to every region in the years 2030, 2050, 2080 and 2100.*

Region	2030 [%]	2050 [%]	2080 [%]	2100 [%]
mex	43	83.29	80.76	83.38
mys	43	100	103.45	106.21
nde	43	98.41	98.37	99.26
nld	43	100	103.45	106.21
noan	43	96.18	97.42	100.59
noap	43	92.94	91.09	95.27
nor	43	100	103.45	106.21
oeu	43	91.87	81.61	78.42
osea	43	100	103.45	106.21
pol	43	100	103.45	106.21
prt	43	100	103.45	106.21
rcam	43	84.1	90.67	100.6
rcz	43	100	103.45	106.21
rfa	43	100	103.45	106.21
ris	43	100	103.45	106.21
rjan57	43	92.71	94.4	97.78
rom	43	92.52	86.59	87.67
rsaf	43	59.36	72.96	84.39
rsam	43	100	102.42	105.18
rsas	43	67.54	75.17	83.29
rsl	43	100	103.45	106.21
rus	43	100	103.45	106.21
slo	43	100	103.45	106.21
sui	43	100	103.45	106.21
swe	43	100	103.45	106.21
tha	43	100	103.45	106.21
tur	43	100	99.42	98.81
ukr	43	96.71	85.77	81.25
usa	43	100	103.45	106.21
vnm	43	100	103.45	106.21
zaf	43	100	97.05	96.65

Table A.2: *Emission control rates of the Welfare solution, referred to every region in the years 2030, 2050, 2080 and 2100.*

Region	2030 [%]	2050 [%]	2080 [%]	2100 [%]
arg	43	100	103.45	106.21
aus	43	100	103.45	106.21
aut	43	100	103.45	106.21
bel	43	88.59	103.45	106.21
bgr	43	74.95	76.34	78.1
blt	43	88.92	103.45	106.21
bra	43	100	103.45	106.21
can	43	100	103.45	106.21
chl	43	92.7	103.45	106.21
chn	43	100	98.83	96.65
cor	43	100	103.45	106.21
cro	43	54.38	56.48	60.36
dnk	43	99.21	103.45	106.21
egy	43	65.8	76.51	82.04
esp	43	77.62	102.46	106.21
fin	43	98.52	103.45	106.21
fra	43	100	103.45	106.21
gbr	43	100	103.45	106.21
golf57	43	68.24	70.51	73.26
grc	43	93.01	103.45	106.21
hun	43	83.36	103.45	106.21
idn	43	93.27	103.45	106.21
irl	43	95.72	103.45	106.21
ita	43	79.76	103.45	106.21
jpn	43	83.91	103.45	106.21
meme	39.6	58.53	67.37	73.86
mex	43	65.32	74.12	80.81
mys	43	83.54	95.56	104.76
nde	43	83.08	100.33	106.21
nld	43	89.84	103.45	106.21
noan	43	74.63	85.74	91.43
noap	43	66.33	77.8	85.01
nor	43	100	103.45	106.21

Continued on next page

Table A.2: *Emission control rates of the Welfare solution, referred to every region in the years 2030, 2050, 2080 and 2100.*

Region	2030 [%]	2050 [%]	2080 [%]	2100 [%]
oeu	43	69.31	71.21	73.17
osea	43	80.62	94.87	104.99
pol	43	100	103.45	106.21
prt	43	78.36	103.45	106.21
rcam	41.82	64.85	83.2	96.16
rcz	43	100	103.45	106.21
rfa	43	91.83	103.45	106.21
ris	43	91.47	91.12	88.89
rjan57	43	76.89	94.56	104.36
rom	43	67.04	72.97	77.23
rsaf	19.4	49.9	76.9	90.9
rsam	43	82.47	94.06	100.15
rsas	26.29	53.55	74.46	85.24
rsl	43	85.89	103.45	106.21
rus	43	100	103.45	106.21
slo	43	75.64	101.03	106.21
sui	43	96	103.45	106.21
swe	43	92.23	103.45	106.21
tha	43	87.55	103.45	106.21
tur	43	81.52	84.11	85.72
ukr	43	81.72	81.48	78.85
usa	43	100	103.45	106.21
vnm	43	81.78	97.3	104.88
zaf	43	80.11	85.88	88.38

Table A.3: *Emission control rates of the Temperature solution, referred to every region in the years 2030, 2050, 2080 and 2100.*

Region	2030 [%]	2050 [%]	2080 [%]	2100 [%]
arg	43	100	103.45	106.21
aus	43	100	103.45	106.21
aut	43	100	103.45	106.21
bel	43	99.8	103.45	106.21

Continued on next page

Table A.3: *Emission control rates of the Temperature solution, referred to every region in the years 2030, 2050, 2080 and 2100.*

Region	2030 [%]	2050 [%]	2080 [%]	2100 [%]
bgr	43	100	103.45	106.21
blt	43	100	103.45	106.21
bra	43	100	103.45	106.21
can	43	100	103.45	106.21
chl	43	100	103.45	106.21
chn	43	100	103.45	106.21
cor	43	100	103.45	106.21
cro	43	100	103.45	106.21
dnk	43	100	103.45	106.21
egy	43	100	103.45	106.21
esp	43	97.04	103.45	106.21
fin	43	100	103.45	106.21
fra	43	100	103.45	106.21
gbr	43	100	103.45	106.21
golf57	43	100	103.45	106.21
grc	43	100	103.45	106.21
hun	43	100	103.45	106.21
idn	43	100	103.45	106.21
irl	43	100	103.45	106.21
ita	43	95.96	103.45	106.21
jpn	43	100	103.45	106.21
meme	43	87.69	103.45	106.21
mex	43	99.92	103.45	106.21
mys	43	100	103.45	106.21
nde	43	100	103.45	106.21
nld	43	99.52	103.45	106.21
noan	43	100	103.45	106.21
noap	43	100	103.45	106.21
nor	43	100	103.45	106.21
oeu	43	100	103.45	106.21
osea	43	100	103.45	106.21
pol	43	100	103.45	106.21
prt	43	95.96	103.45	106.21

Continued on next page

Table A.3: *Emission control rates of the Temperature solution, referred to every region in the years 2030, 2050, 2080 and 2100.*

Region	2030 [%]	2050 [%]	2080 [%]	2100 [%]
rcam	43	100	103.45	106.21
rcz	43	100	103.45	106.21
rfa	43	100	103.45	106.21
ris	43	100	103.45	106.21
rjan57	43	100	103.45	106.21
rom	43	100	103.45	106.21
rsaf	43	77.24	103.45	106.21
rsam	43	100	103.45	106.21
rsas	43	100	103.45	106.21
rsl	43	100	103.45	106.21
rus	43	100	103.45	106.21
slo	43	91.58	103.45	106.21
sui	43	100	103.45	106.21
swe	43	99.08	103.45	106.21
tha	43	100	103.45	106.21
tur	43	100	103.45	106.21
ukr	43	100	103.45	106.21
usa	43	100	103.45	106.21
vnm	43	100	103.45	106.21
zaf	43	100	103.45	106.21

Table A.4: *Emission control rates of the 90/10 solution, referred to every region in the years 2030, 2050, 2080 and 2100.*

Region	2030 [%]	2050 [%]	2080 [%]	2100 [%]
arg	43	100	103.45	106.21
aus	43	100	103.45	106.21
aut	43	100	103.45	106.21
bel	43	100	103.45	106.21
bgr	43	91.78	86.37	85.8
blt	43	100	103.45	106.21
bra	43	100	103.45	106.21
can	43	100	103.45	106.21

Continued on next page

Table A.4: *Emission control rates of the 90/10 solution, referred to every region in the years 2030, 2050, 2080 and 2100.*

Region	2030 [%]	2050 [%]	2080 [%]	2100 [%]
chl	43	100	103.45	106.21
chn	43	100	95.26	88.85
cor	43	100	103.45	106.21
cro	43	72.19	67.3	68.04
dnk	43	100	103.45	106.21
egy	43	72.43	77.25	82.11
esp	43	100	103.45	106.21
fin	43	100	103.45	106.21
fra	43	100	103.45	106.21
gbr	43	100	103.45	106.21
golf57	43	75.06	64.51	62.56
grc	43	100	103.45	106.21
hun	43	100	103.45	106.21
idn	43	95.23	97.89	99.14
irl	43	100	103.45	106.21
ita	43	100	103.45	106.21
jpn	43	100	103.45	106.21
meme	43	69.65	72.19	76.53
mex	43	74.19	72.26	74.55
mys	43	98.35	102.35	106.21
nde	43	76.1	78.2	79.74
nld	43	100	103.45	106.21
noan	43	81.87	85.03	88
noap	43	75.17	75.59	80.46
nor	43	100	103.45	106.21
oeu	43	81.77	73.97	71.39
osea	43	87.53	91.8	100.24
pol	43	100	103.45	106.21
prt	43	100	103.45	106.21
rcam	43	67.52	77.22	88.38
rcz	43	100	103.45	106.21
rfa	43	100	103.45	106.21
ris	43	100	94.53	91.29

Continued on next page

Table A.4: *Emission control rates of the 90/10 solution, referred to every region in the years 2030, 2050, 2080 and 2100.*

Region	**2030 [%]**	**2050 [%]**	**2080 [%]**	**2100 [%]**
rjan57	43	84.06	89	93.5
rom	43	78.47	75.01	76.22
rsaf	20.89	36.5	53.37	66.46
rsam	43	93.73	95.13	98.12
rsas	29.98	41.7	51.17	59.59
rsl	43	100	103.45	106.21
rus	43	100	103.45	106.21
slo	43	100	103.45	106.21
sui	43	100	103.45	106.21
swe	43	100	103.45	106.21
tha	43	100	103.45	106.21
tur	43	94.67	87.83	86.06
ukr	43	87.6	79.56	75.61
usa	43	100	103.45	106.21
vnm	43	86.39	95.03	100.52
zaf	43	94.04	90.32	90.01